Conventional and Advanced Imaging Evaluation of Spine

4

Girish Boraiah and Avneesh Chhabra

History of Spine Imaging

X ray discovery by Roentgen happened in the year 1895. But, the use of Spine x-rays started around 1920s and immediately, it was followed by X-ray tomography. Earliest clinical use of fluoroscopy, then called Cineradiography, was for the evaluation of joint movement in 1905. Subsequently fluoroscopy was incorporated into surgery and also for the evaluation of artificial limb fitted stump. Spine Fluoroscopy was gradually incorporated into intraoperative imaging over the next few years [1]. Use of Spine x-rays to assess trauma, spine instability and screening of many disease entities like infections, developmental aberrations and tumors has retained relevance to this day. Tomography (before being replaced mostly by CT) has the advantage over plain X-rays for the detection of subtle osseous abnormalities, such as complex fractures, bone fragments within the spinal canal, and cortical erosions. Later pneumoencephalography, pneumomyelography and myelogram using Lipiodol type contrast slowly emerged as additional tools to diagnose intracranial tumors, spinal cord tumors and hydrocephalus. For myelogram, thorium dioxide (Thorotrast), iophendylate (Pantopaque) and Meglumine were used for decades with less frequent adverse reactions or severe complications. Subsequently in the early 1970s, less toxic nonionic water-soluble contrast

G. Boraiah
Dr. Chandramma Dayananda Sagar Institute of Medical Education & Research, Harohalli, Ramanagara, Karnataka, India

A. Chhabra (✉)
University of Texas at Southwestern Medical Center, Dallas, TX, USA

Johns Hopkins University, Walton Center of Neurosciences, Liverpool, UK
e-mail: avneesh.chhabra@utsouthwestern.edu

C. E. Noe (ed.), *Multidisciplinary Spine Care*,
https://doi.org/10.1007/978-3-031-04990-3_4

Metrizamide and in 1980s, iohexol and iopamidol came into use. Spinal angiography started around 1970s. Selective catheterization using the Seldinger technique and subtraction technique was developed subsequently for assessing small abnormal vessels and related spinal vascular malformations. Till today, digital spinal angiography remains the study of choice due to an inherent advantage of superior spatial resolution and multiple angiographic runs on table, even though CT (computed tomography) angiography and MR (magnetic resonance) angiography are widely available. First EMI CT scanner introduced in 1973 could image only the head. In 1975, CT imaging of the spine became available followed by introduction of post-myelographic CT. In early 1980s, Lumbar spine CT with contrast was extensively used in post-operative/degenerative spine disease, tumors and infection assessment. Even with low field, 0.15 T–0.6 T MRI scanners in the early 1980s, the contrast resolution was superior to the best available CT scanners at that time. With the introduction of intravenous Gadolinium based contrast agents (GBCA) in 1988, the spinal cord and its pathology were better visualized on contrast enhanced MRI than CT, despite the fact that only low field magnets were available. Ultrasound was also gaining popularity and it was prudently used for spinal assessment in infants for meningocele, tethered cord, etc. Ultrasound has though limited role in adult spine imaging [2].

With advances like 3D (dimensional) imaging, dual energy CT scanning, metal artifact reduction techniques, fast scanning machines / techniques, low dose scanning (using automated iterative approaches and dose modulation), dynamic contrast scanning and so on, the capabilities of CT imaging have been at the new frontiers. Intra-operative CT and CT fluoroscopy have been made real-time imaging possible with excellent surgical and interventional radiology planning. Even with such advancements, the main drawbacks of CT are radiation exposure and poor soft tissue contrast, when compared to MRI. Hence, MRI with latest technology like 3-T (tesla) imaging, multi-channel spine coils, metal artifact reduction, fast scanning techniques with turbo spin-echo, 3D imaging, motion studies using gradient-echo sequences, echo-planar imaging, and parallel imaging, etc. has become the first choice for advanced spinal imaging in almost all conditions. Newer sequences like DWI (diffusion weighted imaging), DTI (diffusion tensor imaging), CSF flow studies, MR Neurography (MRN), MR spectroscopy (MRS), and perfusion MR imaging have provided abundance of imaging details, which were not otherwise possible. Navigational MRI systems are also being exploited similar to CT imaging for assistance with robotic and interventional procedures [3].

This chapter will focus on the commonly used imaging modalities for the evaluation of spinal pathologies so that the reader can learn their appropriate indications and role in different spinal conditions. Imaging appearances of various pathologies are discussed with relevant case examples. Finally, advanced and emerging imaging modalities in the domain of spine imaging are also highlighted.

Morbidity Related to Spine

By Medical Expenditure Panel Survey, approximately 6% of US adults reported an ambulatory visit for a primary diagnosis of a back or neck condition (13.6 million people in the year 2008). Between the years 1999 and 2008, the mean inflation adjusted annual expenditures on medical care, chiropractic care, and physical therapy (three of the most common ambulatory health services utilized by individuals with spine conditions) for these patients increased by 95% (from $487 to $950 per patient per year). Approximately $90 billion is spent on the diagnosis and management of low back pain, and an additional $10 to $20 billion is attributed to economic losses in productivity each year.

The frequency of ambulatory visits for Intervertebral disk disorders, sprains and strains, and for disease related to spinal curvature is at 18.7%, 7.0%, and 2.8%, respectively [4]. The 2010 global burden of disease study estimated that low back pain is among the top ten diseases and injuries that account for the highest number of disability-adjusted life years (DALY) worldwide.

Imaging Evaluation

Following a through clinical assessment, radiography is the first line screening modality. This may be supplemented with fluoroscopy as needed. Advanced imaging with CT and MRI is indicated in specific circumstances, as outlined in the subsequent sections.

Radiographic Evaluation of Spine

The radiographic (X-ray) imaging of cervical, thoracic and lumbosacral spine is commonly performed using frontal (anteroposterior, AP), lateral, and bilateral oblique views. X-rays serve as the first and cost-effective screening modality for spinal evaluation in almost all conditions, except in emergent post-traumatic assessment where CT might be chosen as the initial screening modality. AP view allows optimal assessment of the scoliosis, vertebral count, lumbosacral transitional vertebra (LSTV), transverse process fracture, pedicular involvement/injury, paravertebral soft tissues, uncovertebral joint, and sacroiliac (SI) joint disease. Lateral view is optimal for the evaluation of spinal curvature, sagittal balance assessment, evaluation of short pedicles, vertebral compression and spinal process fractures, vertebral retropulsion, Baastrup's disease, spinal listhesis, atlanto-axial dislocation and prevertebral soft tissues. Oblique views are optimal for facet joints, spondylolysis, SI joint, and neural foraminal assessment. Libson et al. concluded that 20% of pars interarticularis fractures (spondylolysis) were detected only on the oblique views

[5]. Special X-ray views are obtained for different regions and various indications, e.g. bending views for scoliosis, and flexion and extension views for listhesis and potential spinal instability. More than 2 mm anteroposterior motion and asymmetrical disc narrowing are indicators of anteroposterior and rotational instability, respectively. Anterolisthesis is graded from I to IV based on 4 quarters of end-plate widths of the inferior vertebra, e.g. grade IV anterolisthesis is >75% slippage of the vertebra. Spondyloptosis is referred to as Grade V by many. More than grade II anterolisthesis usually has spondylolysis in association. Retrolisthesis is graded from I to III based on degree of neural foraminal stenosis in thirds, i.e. mild, moderate, or severe stenosis correspond to the grade I–III. LSTV is classified based on Castellvi classification into class I–IV. The diagnostic standard for Lumbar segmental instability (LSI) is excessive translational or rotational movements between lumbar vertebrae, accomplished by using functional (flexion–extension) radiographs, with development of 2 mm or more listhesis or more than 5–10° of rotation component, the latter is though more difficult to identify.

In the cervical spine, main features to evaluate are vertebral body height, transverse processes, overlapping articular processes of facet joint, uncovertebral joint, equal intervertebral spaces, centrally placed spinous processes and medial ends of upper ribs. Also visible are soft tissues mainly muscles, lung apices and the central air-filled trachea. Less than or more than 50% anterolisthesis is associated with unilateral or bilateral facet dislocations, respectively. The 1st (atlas) and 2nd (axis) cervical vertebrae are best assessed on the open mouth view. Open mouth view is an AP projection which shows central odontoid peg of the axis, bilateral lateral masses of atlas along with bilateral atlantoaxial joints equidistantly placed from the midline (peg) (Fig. 4.1). Open mouth view can identify C1 burst (Jefferson's) fracture, C2 Odontoid (Dens) fracture), alar or transverse ligament injury and basilar invagination. Fuch's view of the Odontoid process can be used as an alternative in cases with no history of acute spinal injury. If there is widening of one side, say right sided lateral atlantoaxial space, it should correspond to rotation of the face towards right

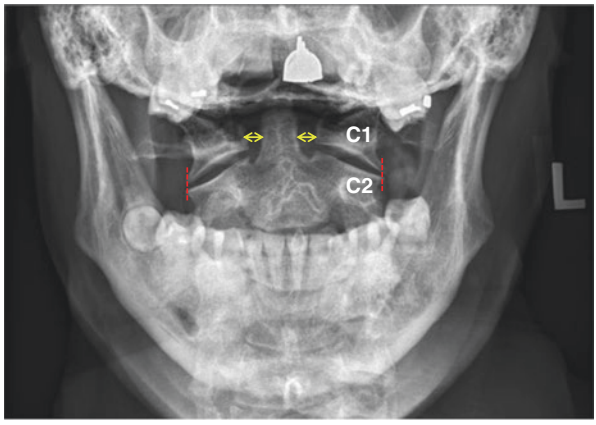

Fig. 4.1 Open mouth view. Equal distance between dens to ring of C1 on either side (↔). Normal alignment of lateral margins of C1 and C2 (red lines)

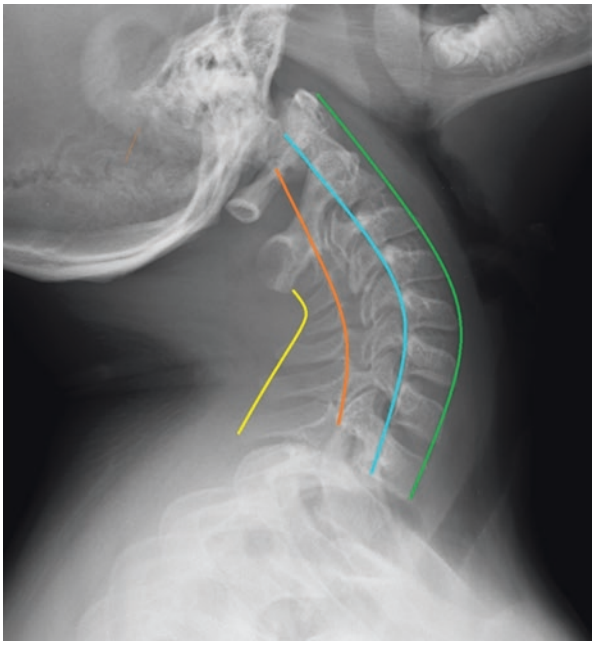

Fig. 4.2 Cervical spinal contour lines. 1. Anterior vertebral line (Green). 2. Posterior vertebral line (Blue). 3. Spinolaminar line (Orange). 4. Posterior Spinous line (Yellow)

side. If the face is rotated to the other side, rotary subluxation diagnosis can be confirmed.

Lateral view shows the prevertebral soft tissue thickness/space (it is abnormal if it measures >7 mm at C2 level and >22 mm in adults or >14 mm in children (<15 years) at C6, or is roughly larger than the corresponding vertebral body width or if there is focal dense soft tissue bulge at any level), atlantoaxial interval (normal is up to 2.5 mm in adults and 5 mm in children), intervertebral spaces, continuous C2 ring (Harris ring), spinous processes, dens, anterior arch of the atlas, facet joints with superior and inferior articulating surfaces. C2 vertebra has the largest body and C3 represents the reference vertebral height to compare for the evaluation of compression fractures. C7 has the largest spinous process. Look for parallelism of the facet joint articulations. It is important to note four spinal contour lines to evaluate instability or malalignments, especially in the trauma setting (Fig. 4.2). Step-off in the contours of these lines is pathologic except in pseudolisthesis, which can be seen at C2–3 and C7–T1 levels.

1. Anterior vertebral line connecting the anterior margins of the vertebrae.
2. Posterior vertebral line connecting the posterior margin of the vertebrae.
3. Spinolaminar line connecting the confluence of bases of the spinous processes and the posterior margin of laminae, depicts the posterior margin of the spinal canal. This line represents the most important line during alignment evaluation as it is not disrupted in pseudolisthesis.

4. Posterior Spinous line connecting the posterior margin of the spinous processes. If space between spinous processes is widened, it suggests interspinous ligamentous injury in setting of trauma.

Os odontoideum is a congenital variant of the axis, which is variable in size and shape, well corticated, smooth and separate from rest of short odontoid process. It can be identified and differentiated by X-rays with the open mouth, anteroposterior, and lateral views. Dynamic lateral flexion and extension views may provide information about atlanto-axial instability. CT/MRI may be necessary in few cases to glean additional information [7]. Atlantooccipital assimilation is a partial or complete congenital fusion between the atlas and the base of the occiput, which often requires CT for complete evaluation [8]. If apex of dens breaches the plane of the foramen magnum, then basilar impression is suspected. When the dens protrudes above the foramen magnum, a basilar invagination is diagnosed, which can result in chronic headaches, limited neck motion, and acute neurologic deterioration [9]. These entities are optimally assessed by CT/MRI. Craniometry [10] through MRI plays a crucial role in evaluation and management of these craniovertebral junction anomalies.

Denis [11] divided spine into three columns to assess spine instability secondary to trauma, which was an improvisation of the prior two column classification from Holdsworth (1970). Anterior column comprises anterior half of vertebral body, anterior half of annulus fibrosus and anterior longitudinal ligament. Middle column comprises posterior half of vertebral body, posterior half of annulus fibrosus and posterior longitudinal ligament. Posterior column comprises posterior bony arch of vertebra, supraspinous ligament, interspinous ligament, ligamentum flavum and facet joint capsule. Involvement of two or more columns is associated with instability and reduced load carrying capacity (Fig. 4.3) [12]. A lateral spine x-ray can identify 75% of fractures with a sensitivity of 85%. The sensitivity increases to over 90% when a full series of AP, lateral, oblique and open mouth X-rays are obtained (Fig. 4.4) [6]. Cervicothoracic (swimmer's view) lateral projection of cervical spine with arm by side of the head allows better visualization of C-7, T-1, and T-2 vertebrae due to uncovering of the spine from the bony and soft tissues of the shoulder girdle (Fig. 4.5).

Radiography in Scoliosis

Angulation of the lateral spinal curvature with Cobb angle of 10° or more is referred to as Scoliosis. If Cobb angle is less than 10°, it is called spinal asymmetry. Frontal X-rays are used to grade the vertebral rotation by Nash-Moe method, to measure coronal balance and to evaluate Cobb angle (Figs. 4.6 and 4.7). Cobb's angle changes with standing frontal, supine rightward- and leftward-bending radiographic views. These views along with standing lateral view (used to measure sagittal balance) are employed to classify scoliosis by Lenke system, which is widely used in guiding surgery. Another study by Alberto Ofenhejm Gotfryd et al. suggested using

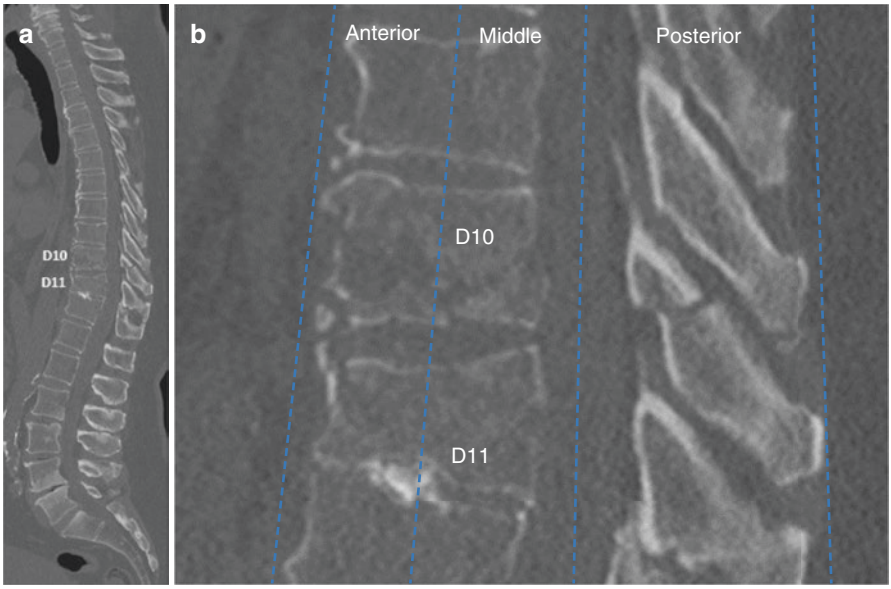

Fig. 4.3 Three column fractures of the spine involving D11 and D10 respectively, on sagittal CT. (**a**) shows sagittal reconstruction from 3D CT and (**b**) shows zoomed view of the fractures at D10/11 level

a lateral oblique view radiograph in supine position to predict the percentage operative correction achievable using pedicle screws for the main thoracic curve, in patients with Adolescent idiopathic scoliosis of Lenke types 1A and 1B. For idiopathic scoliosis in adolescent and adults with Cobb angles of less than 20° and 30° respectively, follow-up imaging at 4–12-month intervals suffices. Bracing and surgery are generally opted when the Cobb angle is between 20° to 45° and greater than 45°, respectively. Such therapeutic decisions are also based on the age and scoliosis progression [13].

In a study by Hasegawa et al. [14] showed that in x-ray and CT imaging, the measurements (Pelvic tilt, pelvic incidence, Cobb and rotation angles of the major curve) especially of the thoracolumbar area, were significantly greater in the standing position than in the supine position. Whereas the sacral slope was significantly smaller in the standing position than in the supine position.

Digital Video Fluoroscopy

Digital video fluoroscopy (DVF) to assess normal and abnormal lumbar spinal motions in vivo has been suggested by many as being superior to the static flexion–extension views [15]. Lumbar flexion-extension motion has been assessed with simultaneous use of electrogoniometer and videofluoroscopy. Cost and practical feasibility renders flexion-extension radiography being preferred over

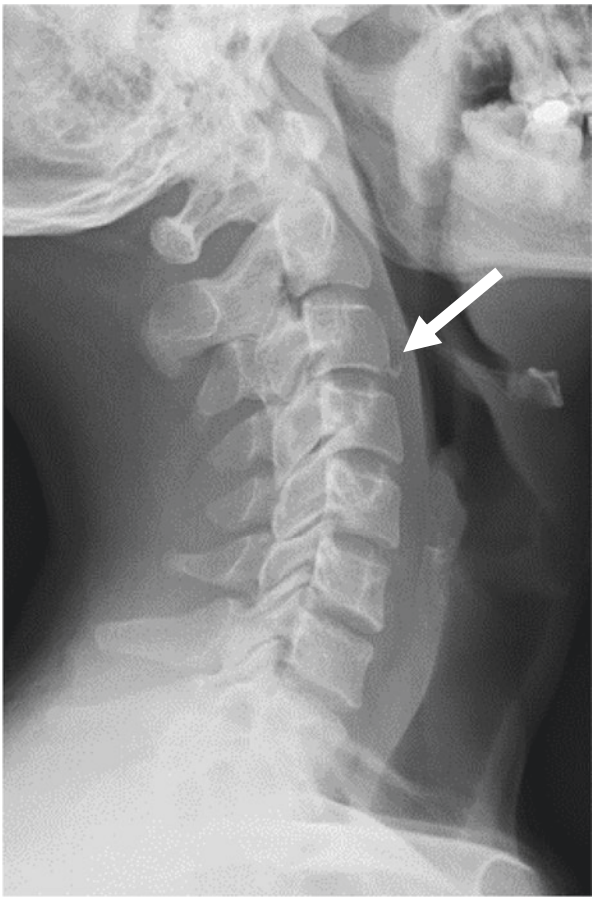

Fig. 4.4 Extension teardrop injury at C3 – Most often, it is a stable injury (arrow)

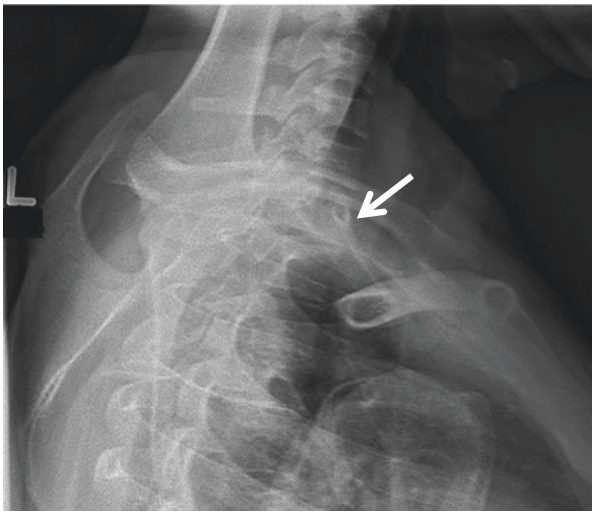

Fig. 4.5 Swimmer's view enables good visualization of the cervicothoracic junction

Fig. 4.6 Whole spine X-ray for scoliosis assessment. Major rotatory dextroscoliosis centered in the mid-lower thoracic spine

video-fluoroscopy. Flexion-extension radiographs have limited utility in the acute setting with high false-negative and false-positive rates [16]. A study comparing flexion-extension radiographs with CT also concluded that they are not efficacious when a negative CT has been performed in blunt trauma without neurological findings [17]. Dynamic fluoroscopy also does not identify additional fractures or instability that has not been identified on CT imaging [18].

Various forms of fluoroscopy have been in use for a long time in orthopedic surgery, especially during spinal surgery. Earlier form of fluoroscopy was with x-ray tube with fluorescent screen [19] and later X-ray Image Intensification with Television became available in the late 1950s [20]. Mobile C-arm image amplifier with television fluoroscopy became available around 1975 [21]. Recently automated C-arm positioning by deep learning process has been shown to improve accuracy on synthetic images derived during the procedure [22].

Fluoroscopy has now become part and parcel of many spine surgical procedures especially spine fixation [23], facet or epidural injection, cage placement and vertebroplasty. Fluoroscopy aids in radiological visualization of the bony structures and instrumentation allowing minimal invasiveness, and thus doing away with direct operative visualization / large operative exposure of the tissues. Fluoroscopy-based procedures have led to safer procedures, shorter procedural time, reduced blood

Fig. 4.7 Whole spine X-ray for scoliosis assessment. S-shaped scoliosis curvature of the thoracolumbar spine and major levoscoliosis of the mid-lower lumbar spine

loss, and early recovery of patients (Fig. 4.8). Main drawbacks of fluoroscopy are steep learning curve for the beginners and radiation exposure, especially to personnel who are involved in long duration procedures or multiple fluoroscopic procedures routinely [24, 25]. With newer technology in fluoroscopy like isocentric 3D C-arm or O-arm with computer-based navigation system in one pass, it is possible to provide 3D reconstruction of the spine, and the image acquisition could be done without the staff being in the operative room, thereby limiting the radiation exposure [26]. These systems have been shown to decrease the overall procedural time while reducing the radiation exposure to the staff [26–29].

Transforaminal extradural and interlaminar epidural steroid and /or anesthetic injections are used to treat cervical radiculopathy (Fig. 4.9). Similarly, radiofrequency ablation (RFA) of medial branch of the spinal dorsal ramus aka Facet joint denervation / rhizotomy, and intra-articular facet steroid injection addresses facetogenic pain. According to one study, fluoroscopically guided lumbar spine epidural injections led to inadvertent intravascular injection in 12%, and it was more common with transforaminal injections [30]. Similarly cervical fluoroscopy guided transforaminal injections was associated with some complications including epidural hematoma [31]. Many studies have provided sufficient evidence to state that

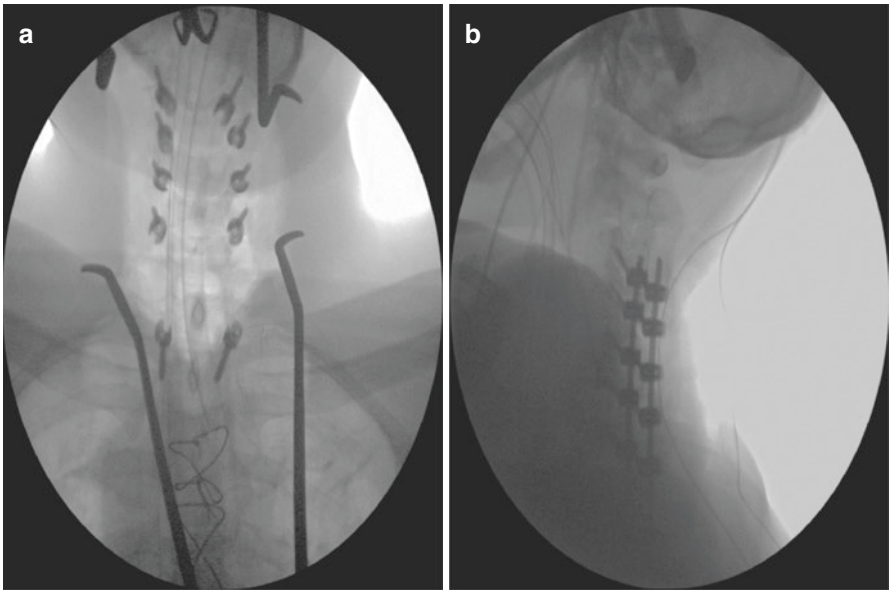

Fig. 4.8 C-arm fluoroscopy of intraoperative cervical spine fixation (**a**) shows pedicular screws with tissue retractors in the middle of fixation procedure and (**b**) shows confirmation of position of rods with screws at the end of fixation

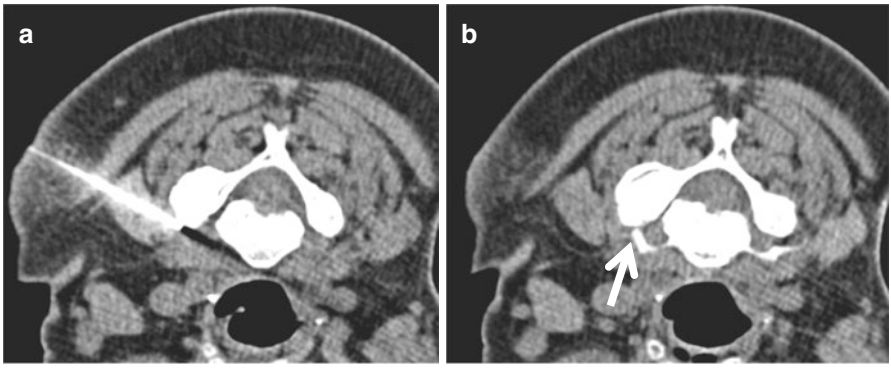

Fig. 4.9 CT guided transforaminal epidural cervical spinal injection (**a**) shows needle tip in epidural space and (**b**) shows contrast spread in epidural space (arrow)

CT guided approach to these injections is safer and effective, though more expensive (Fig. 4.10) [32–35].

In cervical transforaminal injection, the needle tip needs to be placed in junctional location between the foraminal zone and extraforaminal zones. For facet joint injection, needle trajectory should match the joint line curvature (Figs. 4.9 and 4.10). For medial branch block or RFA, the needle needs to be placed between the superior articular process and transverse process.

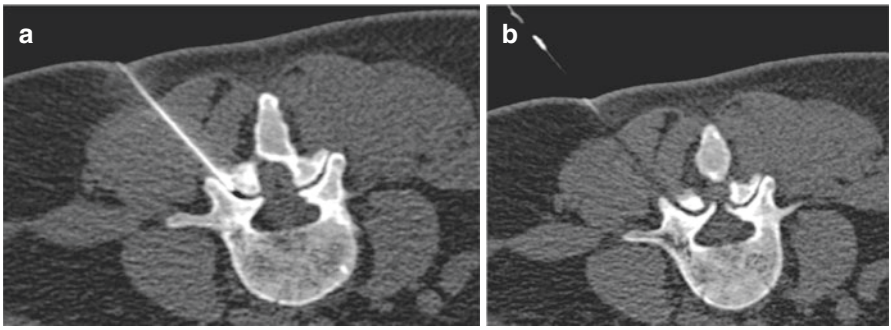

Fig. 4.10 CT guided cervical facet joint injection. (**a**) shows needle tip in facet joint and (**b**) shows minimal contrast in joint space

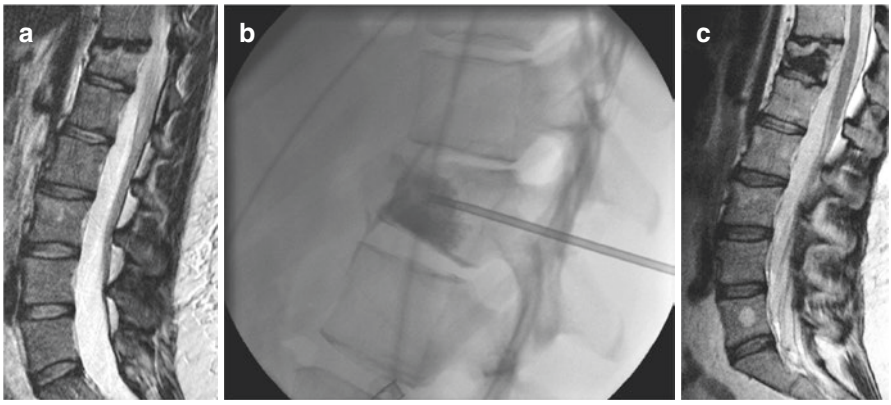

Fig. 4.11 Cementoplasty of wedge compression (**a**) wedge compression of T12vertebra with a hemangioma that deteriorated over months, (**b**) shows fluoroscopic cementoplasty using a 13-gauge Osteo-Site needle via transpedicular approach and (**c**) shows maintenance of height even after 7 years after cementoplasty. Newly formed hemangioma of L5 can also be visualized

Percutaneous cementoplasty or vertebroplasty replaces part of the diseased vertebral body with acrylic cement (polymethylmethacrylate [PMMA]). This prevents vertebral body collapse and its untoward consequences like exiting nerve root compression or sometimes impingement of the spinal cord, thereby alleviating pain. Percutaneous cementoplasty was first performed by Deramond et al. in 1984. Relevant indications for this procedure are severe painful osteoporosis, painful vertebral body / sacral tumors and acetabular tumors, and symptomatic vertebral angioma (Fig. 4.11). During cementoplasty, PMMA polymerizes releasing energy as heat and, also by its cytotoxic nature coagulates the adjacent tumoral cells. Bleeding and infection are the main contraindications. Other complications include cement leak into spinal canal or adjacent veins, infection, post-procedural pain, adjacent segment fractures, and allergic reactions [36].

Discography is a method in which contrast is injected into intervertebral disk using a fine needle, which can reproduce the patient's back pain. The assumption is that if the disc disease is the cause of back pain, then injection of contrast would recreate the pain by stimulating the nerve innervating the annulus fibrosus. CT or MRI based discography can also be performed using corresponding contrast for injection. Whereas fluoroscopy-based discography shows leak and location of the tear, CT and MRI also demonstrate anatomical details of the tears, which might be useful for treatment and surgical planning. Discography was first described by Swedish radiologist Lindblom in 1940s to assess the primary discogenic source of back pain. Main drawbacks for discography are duration involved in the procedure, radiation (if Fluoroscopy or CT used), low diagnostic sensitivity as per many studies, and a complication rate of about 2% for lumbar and 13% for cervical discography. Discography has also been advocated prior to surgery (nucleotomy, spondylodesis) where clinical and imaging could not accurately identify the level of a disc pathology as the causative factor of the back pain and is also used to differentiate scar tissue from recurrent disc prolapse [37–40]. It is however well known that back pain is a result of chronic degenerative changes of the intervertebral discs that occurs at multiple levels, and discography might not be able to identify the exact level for maximal pain. Though MRI identifies many aspects of the disc disease, such pathologies might not translate into defining the cause of pain.

Computed Tomography (CT)

CT is an important modality for the diagnosis of multiple diseases of the spine with a predominant current role in trauma. CT detects subtle fractures, canal / foraminal stenosis, retropulsed bony fragments within canal / foramina, osteophytes, subluxation, spondylolysis, spondylolisthesis and multiple other bony pathologies in an acute setting of trauma. Main advantages of CT lie in capability of 3D reconstruction in multiple planes with better visualization of bony structures than MRI (Figs. 4.3, 4.12, and 4.13). Another important advantage of CT especially in scenario of trauma is faster acquisition and ability to do high resolution angiogram concomitantly. Main drawbacks of CT are radiation exposure, and suboptimal evaluation of the spinal cord, ligamentous and soft tissue structures. Thus, CT plays a key role in spine trauma to achieve early diagnosis and aids in instituting early management. CT also complements MRI in subacute setting and provides additional information e.g. about calcific changes and bony structures, which may be crucial for treatment and pre surgical planning. CT with metal artifact reduction techniques might be better than MRI in assessing spine for bony structures, implant and canal size after spine instrumentation (Fig. 4.12).

CT imaging of the thoracolumbar spine can be concomitantly obtained when thorax or abdomen-pelvis imaging is done in trauma patients for possible visceral, soft-tissue or vascular injuries. Separate dedicated thoracolumbar imaging is not required and bone window reconstruction from abdominothoracic trauma protocol

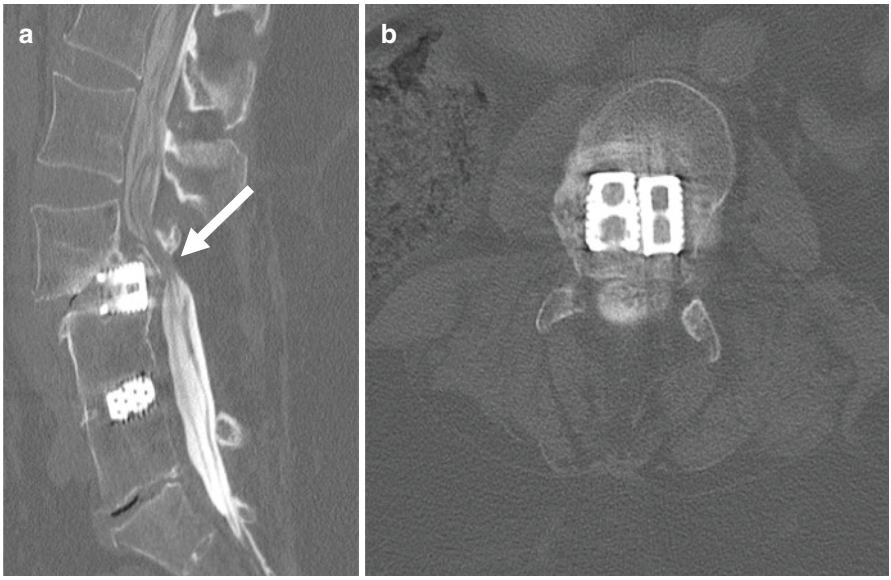

Fig. 4.12 CT myelogram with metal reduction technique. (**a**) Sagittal reformat and (**b**) axial image shows thecal sac narrowing (arrow) at L3–L4 with anterolisthesis and interbody spacer despite spinal decompression. There is no evidence of CSF leak

delivers a sensitivity of 98% and specificity of 97% for the detection of spinal fractures [41]. CT findings in posterior column distraction and potentially unstable posterior ligamentous complex injury includes compression fracture with loss of more than 40% vertebral body height, more than 25° kyphotic angle, interspinous distance widening, posterior column fractures with horizontal orientation, facet joint diastasis, facet joint subluxation or facet joint dislocation. Abdominal hollow visceral injury, mesenteric injury and seat belt injury are often associated with chance-type and transverse process fractures, which may be missed unless evaluated using multiplanar reconstructions [42].

To reduce implant related artifacts and achieve better images, several modifications and techniques are used during CT imaging, including higher peak voltage (>120–140 KVp), higher tube current, lower pitch, smooth reconstruction kernels, metal artifact reduction reconstruction algorithms and dual-energy data acquisition with virtual monoenergetic extrapolation postprocessing. Immediately after spinal instrumentation surgery, CT is performed to assess the proper reduction of fracture, implant placement and also to rule out significant hematoma (which can compress on spinal cord or other important neural structures). Short term or long term follow up with CT is done to evaluate the implant itself, its position, osteolysis around and changes in adjacent soft tissues including collection / particle disease (adverse local tissue reaction) (Fig. 4.12). Though soft tissue can be best evaluated by MRI, initial evaluation for infection and other changes in soft tissue can be best done with CT with lesser artifacts. Variable position of the implant can lead to varied adverse

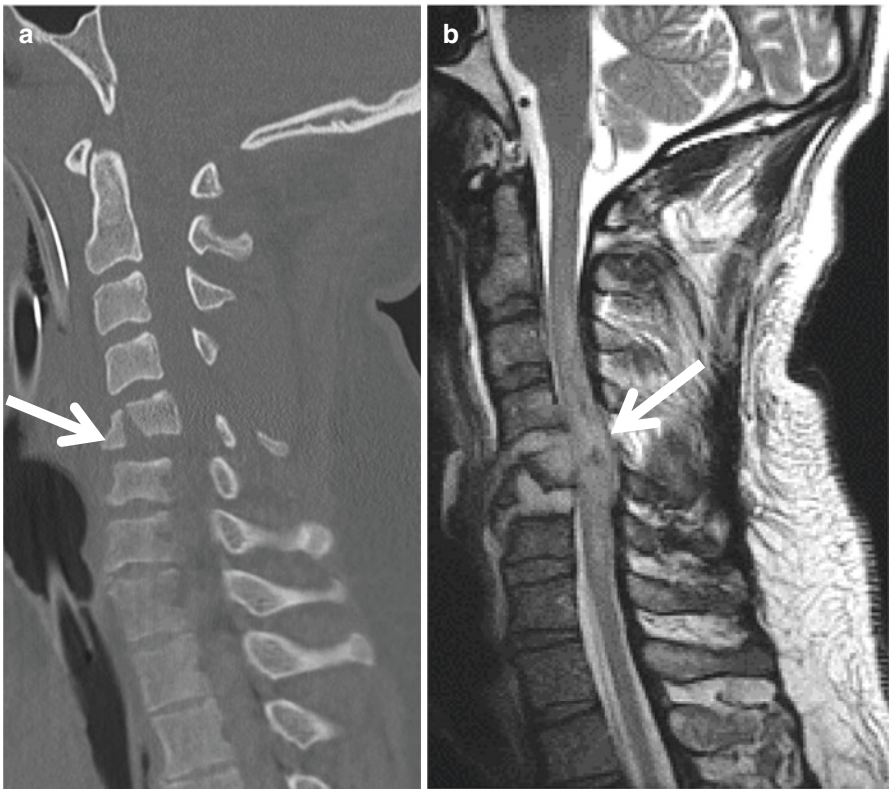

Fig. 4.13 Flexion teardrop injury at C5 – Most often, it is unstable (associated with hemorrhagic spinal cord in this patient, arrows)

outcomes and symptoms based on the position of the implant in relation to the adjacent important structures like thecal sac, neural elements and other soft tissues. Implant failure can occur due to altered dynamics or repetitive stress leading to fractures and / or disengagement of fixation construct [43].

CT myelography even though invasive, has advantages over conventional MR in its ability to obtain dynamic images, postoperative imaging for metallic implant related complications, evaluate slow cerebrospinal (CSF) leaks, superficial siderosis and in cases where MRI is contraindicated. CT myelography best demonstrates the pathologies that contact or narrow the spinal thecal sac or cord (Fig. 4.12), or displace the spinal cord, nerve roots and thecal sac. CT myelography is useful in assessing compressive cystic lesions like spinal arachnoid cysts, spontaneous cord herniation, arachnoid webs, and other intradural cystic lesions. It helps to differentiate such entities and diseases and hence is useful for surgical planning. Filling the arachnoid cyst intrathecally with contrast material also helps exclude neuroenteric cysts. Spinal cord herniation is another important differential to exclude and an absence of CSF ventral or ventrolateral to the cord, lack of CSF loculation dorsal to

the cord, and on postmyelography CT an absence of delayed myelographic CSF opacification dorsal to the cord are important findings that suggest cord herniation rather than an arachnoid cyst [44]. Spinal canal narrowing from Calcium Pyrophosphate Deposition Disease or Ossification of the Posterior Longitudinal Ligament and its effect on thecal sac is also better assessed with CT myelography [45].

CT myelography has disadvantages of being an invasive procedure with risks associated with intrathecal contrast injection, exposure to radiation, and requirement of patient mobilization for contrast to diffuse to the point of interest [46]. Significant spinal extra-arachnoid fluid collections on preprocedural spinal MR imaging can be evaluated with either dynamic CT or digital subtraction myelography [47]. Dynamic CT Myelography is better for assessment of Fast Spinal CSF Leaks [48].

Magnetic Resonance Imaging (MRI)

Role of MRI in spinal imaging is to identify and differentiate pathologies due to vascular, ischemic, infective, inflammatory, neoplastic, demyelination, degenerative, congenital, traumatic and metabolic causes. MRI provides superior soft tissue contrast than other modalities, has multiplanar capability with no radiation exposure, and can specifically demonstrate individual tissue characteristics, such as water, blood, fat, infarction, proton diffusion and perfusion using a multitude of sequences. MRI clearly provides pathologic information about spinal cord, intervertebral disc, ligaments, tendons and paraspinal muscles. It can characterize disc disease into disc bulge, protrusion, extrusion, sequestration, annular fissure and so on (Figs. 4.14, 4.15, and 4.16). Disc dessication is common with aging. In most subjects, lumbar disc levels tend to dessicate beyond the age of 40 years and cervical discs beyond 20–25 years. Disc bulge on MRI demonstrates as extension of the disc material beyond the margins of the vertebra. Posterior disc bulges are important as they can impinge on the thecal sac or the nerve roots. Bulge, by definition, involves more than 90 degrees of the posterior one-half of the disc circumference and is caused by inner annular fissures. Outer annular fissures result in disc herniations, with 45–90° extent, being referred to as a broad-based disc herniation. In general, extrusions and sequestrations of discs are more frequently symptomatic than protrusions. Disc protrusion is broad based and displays obtuse angles with the parent disc on the axial image, doesn't extend beyond the margins of the disc on the sagittal image, maintains dessicated dark T2 disc signal and can demonstrate coexistent annular fissure, which themselves may persist for a long time. Extrusions exhibit a narrower neck with the parent disc, money bag appearance, extend above and below the disc level on sagittal image, are larger, and demonstrate increased T2 signal alteration due to the frequent associated peri-discal inflammatory tissue. The latter can also show rim enhancement on post-contrast images and is also a significant contributor of reduced disc herniation appearance on follow-up MRI with conservative management and physical therapy. Sequestration involves disruption of disc

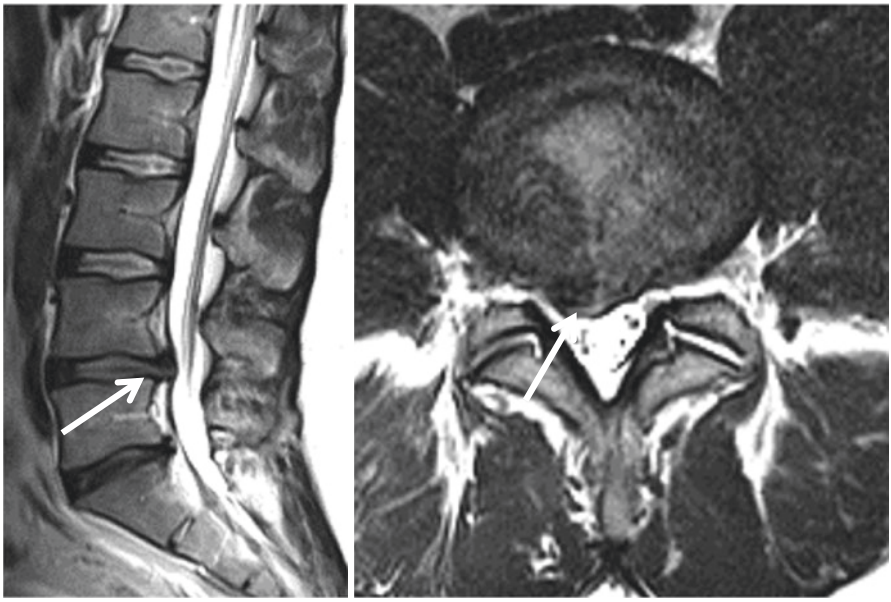

Fig. 4.14 Sagittal and axial T2W MR images show right paracentral disc protrusion

material from the parent disc and superior or inferior migration. Presence of rim enhancement distinguishes it from an extra- or intra-dural tumor (Fig. 4.16). Another important role of MRI is to evaluate the edematous changes in the bone from stress changes. End-plate changes are classically divided into three Modic types (I) edema, (II) fatty metamorphosis, (III) sclerosis, but often, a mixture exists, with edema like T2 signal more associated with pain symptoms. Since, spine spondylosis is part and parcel of normal aging, MRI is also useful to identify coexisting inflammation, infection, or enthesopathy.

MRI has a substantial role in the evaluation of spinal infections. Most common causes include- Staph Aureus, Tuberculosis (TB), Brucellosis and so on, each one with some recognizable patterns of spine involvement. X-rays usually do not provide much information about infection till advanced stage of infection when there is enough destruction of vertebral bone, disc space loss, and significant soft tissue collection/gas formation. CT identification of early infection is suboptimal and often indirect through periosteal reaction, bone erosions, gas formation in soft tissue or sufficient soft tissue collection to be able to identify rim enhancement on contrast study. MRI can identify infection at an early stage by identifying the edema pattern or minimal collection in bone/soft tissue structures. Thin rim contrast enhancement and associated central diffusion restriction suggests infection over neoplasm. Involvement of two adjacent vertebral bodies along with intervening disc and soft tissue phlegmon or abscess (Fig. 4.17) often depicts pyogenic etiology. Multiple vertebral involvements can often be seen in tuberculosis, brucellosis and fungal etiology. Relative sparing of the disc with gibbus formation favors TB. Mixed

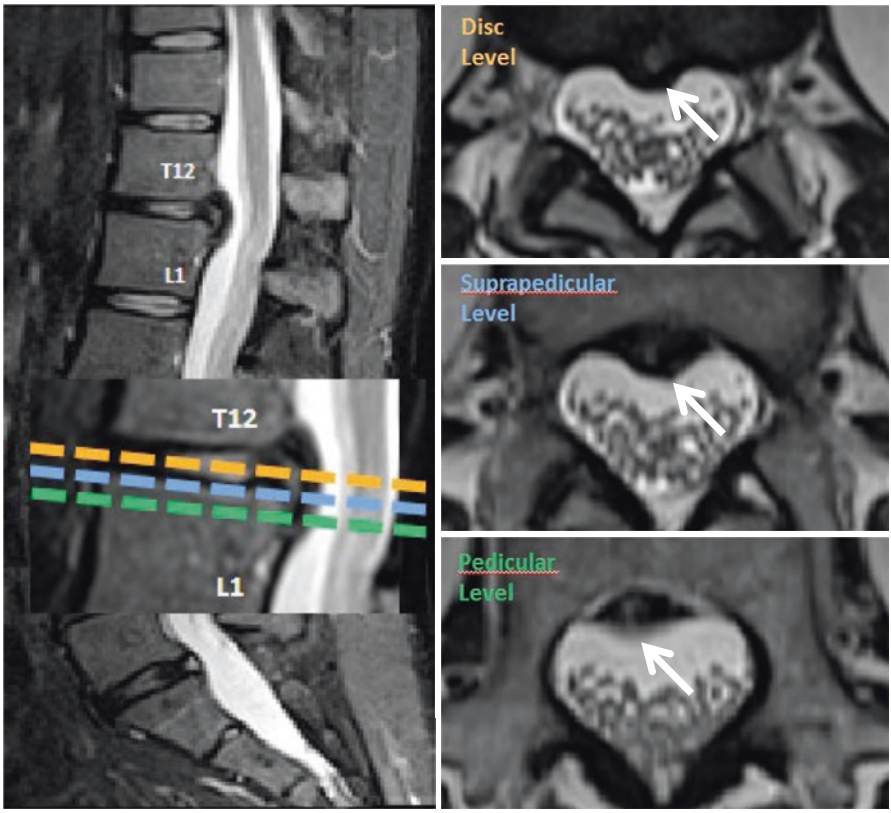

Fig. 4.15 Sagittal and sequential axial T2W MR images show a disc extrusion (arrows) with caudal migration (from disc (Orange) to Pedicular (Green) level)

intensity, less fluidy collections and associated lung lesions or calcification on X-rays favors TB as well. Brucellosis shows involvement of entire vertebral body with sclerosis on plain films and periostitis while gibbus is rare. Hypointense fungal elements in soft tissues along with lytic and sclerotic changes in vertebral body are characteristic of fungal etiology. MRI is useful in finding collections for drainage and can guide the site of biopsy. It is also helpful in follow-up of patients for resolution of infection.

Inflammatory/autoimmune disease of the spine can be distinguished into one involving the spinal cord specifically and the other involving the bony spine. Diseases involving the spinal cord include multiple sclerosis (MS), acute disseminated encephalomyelitis (ADEM), transverse myelitis (TM), neuromyelitis optica spectrum disorders (NMOS) and so on. Inflammatory disease of the bony spine or axial spondyloarthropathy occur specifically secondary to ankylosing spondylitis, psoriasis, lupus arthritis, and rheumatoid arthritis. X-ray and CT overall has no significant role in the diagnosis of inflammatory or autoimmune disease of the spinal cord. In axial spondyloarthropathy, X-ray and CT provide diagnostic and prognostic

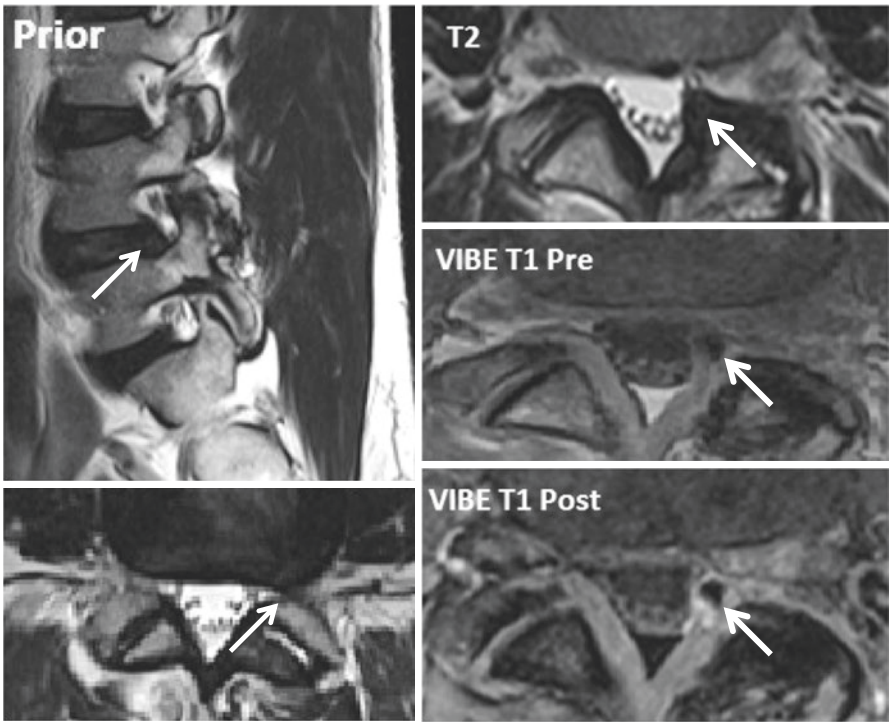

Fig. 4.16 Sequestrated migrated disc material. Extradural peripherally enhancing fragment of extruded migrated disc lying at same level as previous foraminal disc extrusion. VIBE- volume interpolated breath hold examination

information only in the later stages of the disease. MRI remains the cornerstone (Fig. 4.18) of early diagnosis and management of inflammatory / autoimmune disease of both the spinal cord and also the bony spine [49, 50].

Multiple short segment peripheral cord involvement is seen in MS. Whereas long segment holocord involvement is more typically seen in the setting of ADEM, NMOS and transverse myelitis. Using imaging alone, it is difficult to differentiate between multiple sclerosis and NMO. Nonspecific imaging features which support NMO are optic neuritis, less frequent involvement of brain (confluent large hyperintensities in NMOS, when compared to oval lesions in MS), and contiguous long segment central cord involvement. According to one meta-analysis [51] for NMOS, Aquaporin 4 antibody has sensitivity and specificity based on type of assay of about 70 and 95, respectively. TM unlike ADEM does not involve brain, whereas ADEM can involve spinal cord in one-third of the patients. The inflammatory diseases of the spine can be identified with specific enthesopathy patterns (for example, Romanus and Andersson lesions in ankylosing spondylitis reflecting anterosuperior/anteroinferior corner erosions and end plate erosions at discovertebral junctions, respectively), location involved (cervical spine involvement in rheumatoid arthritis and sacroiliac joint in seronegative arthropathies). Use of multiparametric

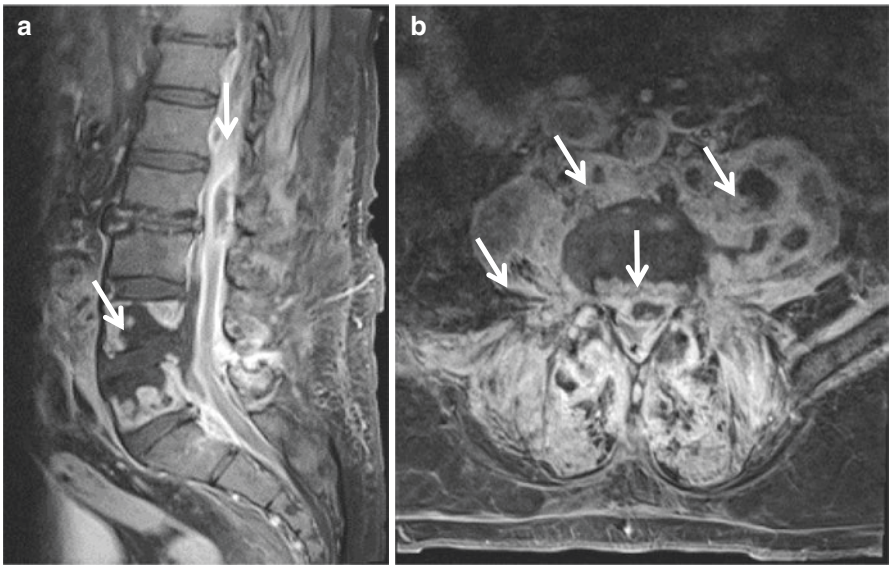

Fig. 4.17 Discitis-osteomyelitis of L4–L5 along with paravertebral abscesses (arrows) and epidural abscesses (arrow-heads) on T1 FS post-contrast (**a**) Sagittal image show the full craniocaudal extent of vertebral involvement and (**b**) Axial image shows epidural phlegmonous and abscess component (arrowhead) compressing on spinal cord

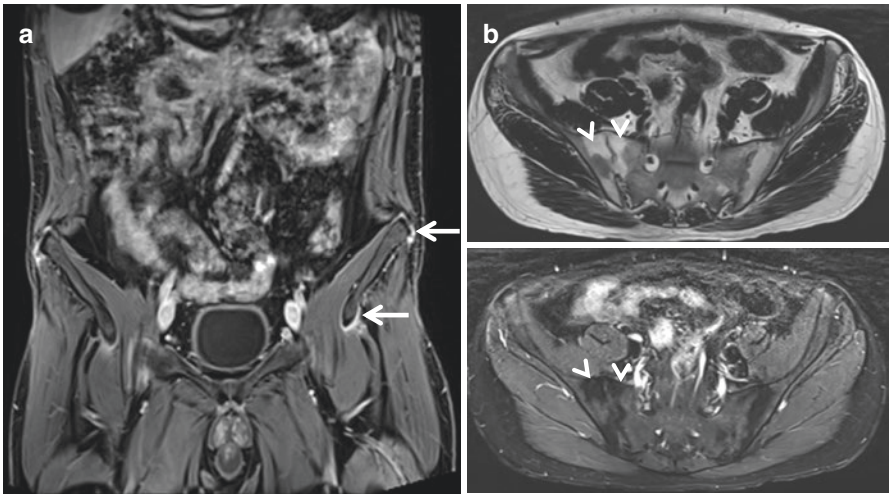

Fig. 4.18 Spondyloarthropathy spectrum (**a**) Coronal T1 FS post-contrast image shows bilateral anterosuperior and anteroinferior iliac spine enhancement of tendinous attachment (arrows) depicting acute enthesitis and (**b**) Axial without and with fat saturation images shows fatty metamorphosis (arrow-heads) and partial ankylosis of bilateral SI joints confirming long-standing spondyloarthritis

and 3D rheumatology lumbosacral MR imaging (MRLI) protocol helps in accurate diagnosis of various stages (acute, subacute and chronic) of inflammatory activity in bones, entheses, ligaments, tendons and joints [49, 50]. Acute lesions typically demonstrate bone marrow edema and chronic lesions show fatty changes/sclerosis. Thus, MRI provides information about the stage of disease and disease activity, which is not only useful in treatment but is also extremely relevant in prognosis and follow-up strategy [52–54].

Tumors of spine may involve the spinal cord (intramedullary, extramedullary and extradural) or the bony spine. Primary neoplasms of the bony spine are rare when compared to the metastatic lesions, except benign hemangiomas. They occur with a incidence of about 5 per 1,00,000 person-years [55]. Most of the primary bony spine neoplasms are benign, most common being enostosis and hemangioma. The incidence of spinal cord tumors is less (Less than 1 per 1,00,000 person-years [56]) compared to the bony spinal tumors. Most common spinal cord related tumors being glioma and ependymoma, and the intra-dural mass lesions include- meningioma and schwannoma/neurofibroma. On radiography, while bony lesions can demonstrate typical missing pedicle of metastasis, punched out lesions of myeloma, corduroy appearance of hemangioma, and sclerotic metastases of prostate cancer, etc.; for spinal cord tumors, x-ray provides only indirect evidence in some tumors due to scalloping and erosion of the bony spine. CT for bony spinal tumor adds more information compared to x ray by providing additional details about matrix characteristics throughout the tumor including calcification of chondrosarcoma, and ossification of osteosarcoma, as well as details of gross dimension of the tumor and bony spinal canal narrowing. CT is most helpful for pre-surgical planning before spinal decompression and/or fusion as well as for CT guided biopsy. For spinal cord tumors, CT provides suboptimal evidence of only thickened spinal cord or calcification if present. The modality is inadequate to differentiate tumor from other etiologies, like infection or inflammation. For bony spinal tumors, MRI is better than CT to evaluate the extent of bone marrow involvement (Fig. 4.19) and also provides high resolution details about extraosseous soft tissue and neurovascular bundle involvement. Though MRI provides extensive details about the matrix, it might not provide details about subtle calcification and ossification. Apart from common metastatic, lymphoma and myeloma lesions, typical locations of bone tumors include- vertebral body (T2 bright lesions- hemangioma (Fig. 4.11), chordoma and chondrosarcoma, T2 dark lesion- Giant cell tumor), pedicles (osteoid osteoma <1.5 cm size and osteoblastoma >1.5 cm), posterior elements (chondrosarcoma, osteochondroma, and aneurysmal bone cyst with fluid-fluid levels). MRI helps in localization of tumor into intramedullary (glioma- ill-defined margins, cervicothoracic area location; ependymoma- sharp margins, cystic changes and hemorrhage, cervical and lumbar locations, and hemangioblastoma- cyst with a vascular nodule), intradural-extramedullary (meningioma, peripheral nerve sheath tumor, and angiolipoma) and extramedullary (metastasis, myeloma, lymphoma, etc.). MRI provides comprehensive details about composition of the tumor, accurate dimensions and extent of the lesion.

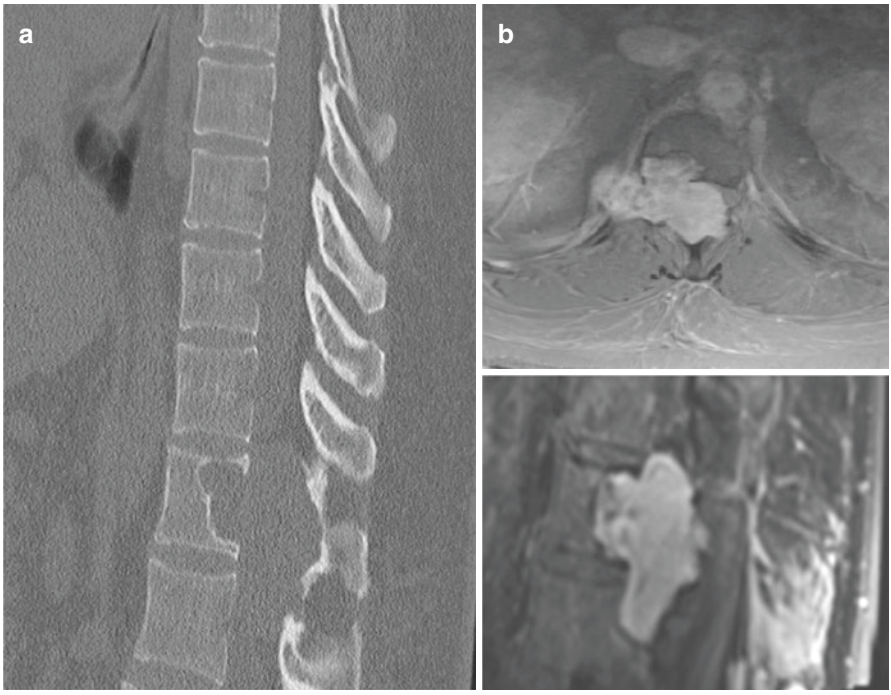

Fig. 4.19 Schwannoma (**a**) Sagittal CT reformat shows vertebral lytic lesion with large intraspinal component and (**b**) T1 FS post-contrast axial and sagittal images however shows homogenous enhancing nerve sheath tumor centered around right neural foramen with dumbbell like extraforaminal and intraspinal component along with anterior vertebral body scalloping

Vascular disorders include vascular malformations, hemorrhage and infarction. Plain x rays provide no significant information in the diagnosis of vascular disorders of the spine (which are rare and constitute about 1–2% of vascular neurologic pathologies) [57]. However digital subtraction angiography (DSA) plays a key role in the diagnosis and management of spinal vascular lesions including arteriovenous fistula and arteriovenous malformation, which are most common such lesions. CT angiogram is useful in the evaluation of hemorrhage and spinal vascular pathologies. CT has no role in spinal cord ischemia (contributing to less than 1% of all strokes) [57]. MRI is the imaging modality of choice for spinal vascular malformation and the angiogram can be obtained using time of flight (2D/3D) and contrast-enhanced sequences. MRI also provides details about congestive spinal cord edema secondary to the vascular malformation and details the soft tissue component of the vascular malformation. Apart from various sequences MRI, susceptibility weighted imaging (SWI) is sensitive in identifying spinal cord bleed and diffusion weighted imaging (DWI) is sensitive in identifying infarctions [57].

Congenital and developmental spine abnormalities range from craniovertebral junction abnormalities to various neural tube anomalies. Congenital bony spine abnormalities can manifest as alterations in normal size and shape of vertebra,

which occur mainly due to variation in fusion of ossification centers, and rarely due to absence of the ossification center itself. Congenital bony spine abnormalities include hemivertebra, butterfly vertebra, block vertebra, spur of diastematomyelia, hypoplasia and aplasia.

Spinal dysraphism is a large set of congenital anomalies secondary to defective neural arch with herniation of meninges or neural elements and associated clinical manifestations. Herniation of neural elements to skin surface can be open (spina bifida aperta) or can be covered by skin, closed (spina bifida occulta) dysraphism. Closed Spinal Dysraphism may go undetected throughout life, as most are asymptomatic. Complex bony spine abnormalities are often associated with spinal cord anomalies [58] and are more common (10 per 10,000 live births) than spinal dysraphisms (3.2–4.6 per 10,000 births) [59]. Ultrasound when performed prenatally, may detect many open neural tube defects as early as 11 weeks and segmentation anomalies of vertebra around 16 weeks. Postnatally, ultrasound is useful in infants, but less so in later ages. Plain x rays can identify congenital bony spine anomalies. CT can identify more subtle bony spine anomalies along with providing some information about soft tissue (especially lipomatous) component of the neural elements. Congenital lumbar canal stenosis (CLSS) and transitional vertebrae (Fig. 4.20) can be identified on CT and MRI [60]. MRI is the imaging modality of choice for spinal dysraphism as it can provide most of the details including the composition of the open neural tube defect and it also helps in identification of subtle entities like neuroenteric cysts, meningeal cysts, syringohydromyelia and so on. MRI is essential in

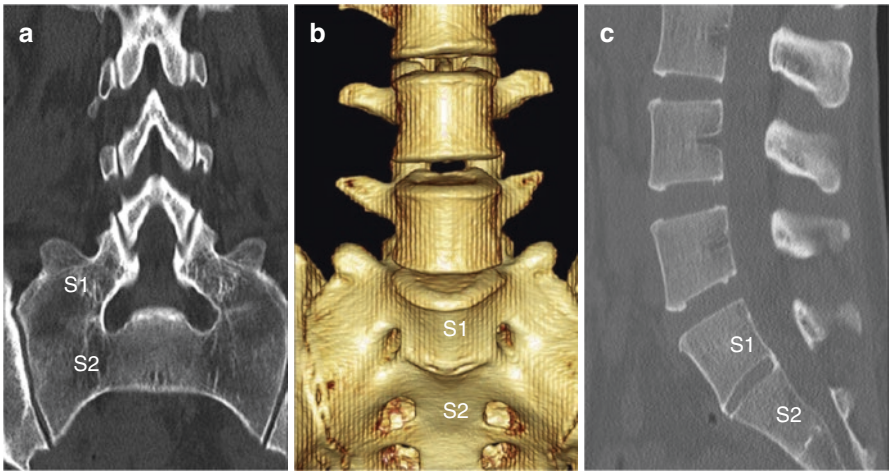

Fig. 4.20 Transverse process of lumbarised S1 (transitional vertebra) fused bilaterally with the sacral transverse process below - Castellvi type IIIb seen on (**a**) CT Coronal reformat, (**b**) Volume rendered image and (**c**) CT Sagittal reformat. (Castellvi types I, II and III depends on transverse processes being large-dysplastic, showing pseudo-articulation with sacrum and complete osseous fusion with sacrum, respectively. Subtypes are further classified unilateral (I/II/III a) or bilateral (I/II/III b). Whereas type IV (with no subtype) is combination of unilateral type II and contralateral type III)

Fig. 4.21 MR myelogram using Coronal heavily T2W steady state sequence shows preganglionic avulsion of the left C7–T1 nerve roots with associated pseudomeningoceles (arrow)

preoperative planning of open neutral tube defects. Fetal MRI is able to identify many of the spinal dysraphisms in utero, differentiate between open and closed spinal dysraphism [61] and also identify fusion anomalies of the spine.

MRI is also the modality of choice for failed back surgery syndrome and other miscellaneous causes of cord abnormalities, such as subacute combined degeneration. Other advances of MR imaging include- MR myelography (Fig. 4.21) and upright MRI. MR myelogram can be performed using heavily T2 weighting or following injection of intrathecal Gadolinium. MR myelogram has uses like CT myelogram and carries other advantages, such as better depiction of neural structures and no radiation. MRI myelography has been shown of value in conditions like tethered cord, adhesive arachnoiditis, disc herniation, spinal arteriovenous malformation, post-traumatic pseudomeningoceles and so on. With improvements in conventional MRI resolution, a common use of myelogram has been to non-invasively detect CSF leak. Off label use of intrathecal gadolinium is also shown to have high rate of detection of CSF leaks compared to CT [47]. The concerns of encephalopathy or seizures after MR myelogram are rare with newer contrast agents [62].

Apart from supine MRI, various other position-based MRI techniques are being evaluated, e.g. (1) Positional MRI (pMRI)-Imaging in varying weight-bearing

positions (e.g. standing, seated or in the positions that worsen symptoms), (2) Kinetic MRI-Static imaging of kinetic maneuvers (e.g., flexion, extension, rotation, lateral bending), and (3) Dynamic MRI with images acquired while the spine is in real-time motion. Serial images played as cine loops nicely show the dynamic movements of the spinal column and pathologic alterations [63, 64]. MRI with neck flexion and extension can reveal dynamic stenosis or Hirayama disease (flexion myelopathy). Upright MRI is believed to replicate the expected effects of body weight and posture has on the spinal curvature and important spinal structures like neural foramina and spinal canal. Recent studies claim that upright MRI can portray occult stenosis, disc protrusion, or instability, which otherwise would have not been clearly assessed in supine MRI. Study by Ferreiro Perez et al. [65] showed posterior disc herniation was underestimated on supine MRI when compared to upright MRI. Similar results of the disc pathology at lumbar spine (L5–S1 followed by L4–L5 and L3–L4) were seen well on upright MRI, as was shown by Gilbert et al. [66]. Meakin et al. [67] showed an increase in curvature under load during upright MRI, when compared against supine MRI. Tarantino et al. [68] showed that dynamic MRI with an open-configuration using low-field tilting MRI system, permits visualization of occult spine and disc pathologies in patients with acute or chronic low back pain who had MRI in the recumbent position or in patients with pain only in the upright position. However, other studies show that no significant difference in various spinal parameters in upright MRI when compared to supine MRI, and thus, the modality has not gained widespread acceptance.

Special MRI Sequences and Applications in Spine Imaging

Diffusion-weighted imaging (DWI) and Diffusion-tensor imaging (DTI) help assess the isotropic and anisotropic diffusion of water molecules respectively, thereby interrogating proton diffusion at a cellular level. DWI renders early visualization and diagnosis of spinal cord and brain infarcts, and identification of small spinal tumors with utmost confidence. Advances in DWI have led to its use in benign and malignant bony spinal lesions, spinal cord lesions, pre and post treatment in infections or malignant lesions. Recently in 2018 Park et al. [69] showed that differentiation of multiple myeloma and metastases is possible with axial diffusion-weighted MR imaging (Fig. 4.22). Daghighi et al. [70] showed that with DWI, it is possible

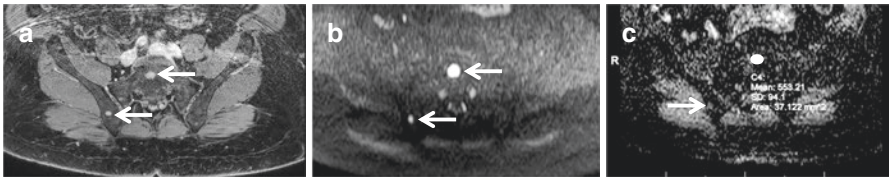

Fig. 4.22 Multiple myeloma (**a**) shows T1 FS post-contrast axial image are seen as discrete enhancing lesions of the sacrum and right ilium, (**b**) shows bright lesions on DWI and (**c**) shows lesions with restricted diffusion (ADC of 0.6×10^{-3} mm^2/s)

to differentiate acute infectious spondylitis from degenerative Modic type 1 change. Significant diffusion restriction is seen with highly cellular, higher grade, and round cell tumors. Pus also restricts as compared to simple fluid collection. Myxoid and chondroid lesions however do not significantly restrict. With evolution of DTI, spinal cord tracts can be evaluated that could provide a road map for conservative surgery to preserve critical (usually motor) neural tracts. DWI of the spine correlates well with the presence or absence of spinal infection and may complement conventional magnetic resonance imaging (MRI) with median ADC value being 740×10^{-6} mm^2/s for patients with positive microbiological sampling and 1980×10^{-6} mm^2/s for patients with negative microbiological sampling ($p < 0.001$) [71]. DWI and DTI usefulness has also been shown in immune-mediated encephalitis, neuritis and neurodegenerative disorders [72]. Finally, DWI has been shown to be useful in detection and quantification (useful for follow-up) of subtle inflammatory changes in Spondyloarthropathy not seen on other MR conventional images (Fig. 4.23) [52–54, 73].

MR Neurography (MRN) is an imaging dedicated to diagnosing peripheral neuropathy and is being rapidly used for characterizing neuromuscular diseases. With advances in fat suppression, fast MRI techniques, 3 T MR scanners and 3D imaging; rapid acquisition of images without temporal degradation in image quality is possible with good isotropic resolution in the range of 0.9–1.5 mm. 3D anatomic nerve-selective MR Neurography results in effective vascular signal suppression and differentiates the nerves from vascular structures within a neurovascular bundle. Fat suppressed 3D DW PSIF (reversed fast imaging in steady state free precession) is one of excellent nerve-selective MRN techniques [74]. Role of MRN has been established in peripheral neuropathy, nerve injury, nerve sheath tumor, nerve entrapment or impingement. MRN also has been used to exclude neuropathy in pathologies mimicking neuropathy and to provide imaging guidance for perineural medication injections [75]. MRN has a significant role in anatomically complex brachial [76] and lumbosacral plexus pathologies [77]. MRN has been applied in diagnosis, treatment and follow-up of nerve related pathologies due to various etiologies (Fig. 4.24). Recently, the technology has been used in diagnosis of greater occipital nerve neuropathy in patients with unilateral occipital migraines with a

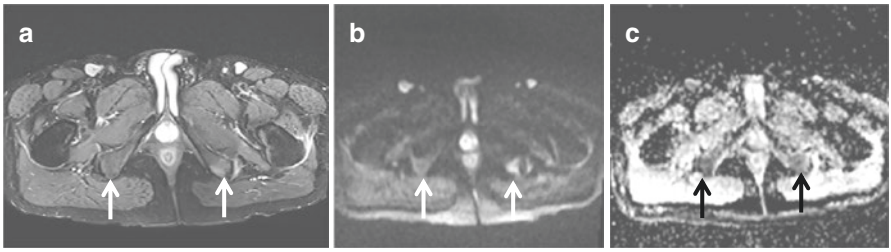

Fig. 4.23 Bilateral (Left > right) ischial tuberosity enthesitis (**a**) shows STIR axial image with subtle edema visible only on left, (**b**) shows bright signal bilaterally on DWI and (**c**) shows altered diffusion bilaterally

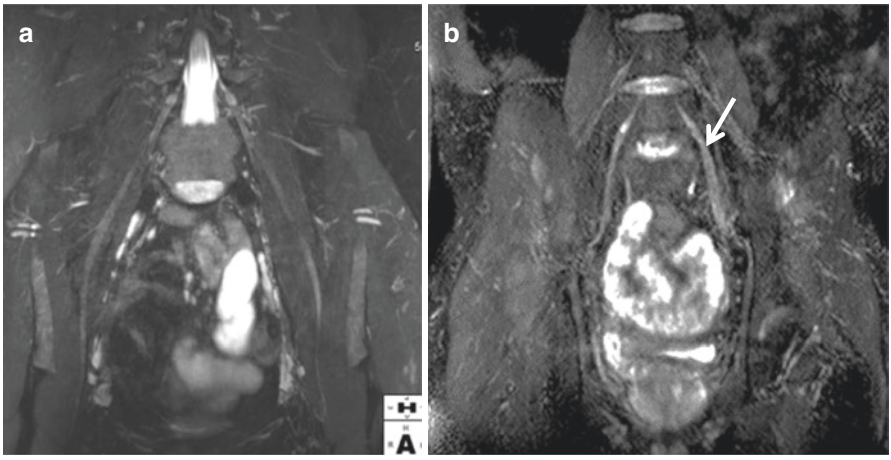

Fig. 4.24 Coronal MIP images of 3D STIR in different patients (**a**) shows bilaterally symmetrical normal femoral nerves, (**b**) shows abnormal thickening of left L5 nerve with obscuration of the left dorsal nerve root ganglion in this case of left L5 radiculopathy (arrow)

good correlation of imaging findings to the clinical presentation [78]. One study on MRN of Lumbosacral Plexus in Failed Back Surgery Syndrome (FBSS) has found neuroforaminal stenosis, iatrogenic nerve injuries, and neuropathy in substantial number of patients who had non-contributory conventional spine MRI so that specific treatment approaches could address the issue of FBSS [79]. DTI employed as part of MRN also reveals neuropathy with reduced fractional anisotropy and increased apparent diffusion coefficient of the affected nerves.

CSF flow imaging of the spine using phase-contrast MRI sequence obtains signal contrast between flowing and stationary nuclei by using opposite gradient sensitization at two different time points. The sequence yields signal from the moving nuclei and nulls signal from the stationary nuclei. Using magnitude and phase images, quantitative and directionality assessments can be done. To distinguish motion, this sequence applies anticipated velocity encoding (VENC) which is the expected maximum CSF flow, generally 5–8 cm per second. Lower VENC like 2–4 cm per second is useful to differentiate communicating versus non-communicating arachnoid cysts and is also useful to evaluate VP shunts for possible obstruction. Higher VENC of 20–25 cm per second depicts high velocity CSF flow, as seen within cerebral aqueduct in normal pressure hydrocephalus [66]. As CSF flow is pulsatile and synchronous with the cardiac cycle, either prospective or retrospective cardiac gating yields the best imaging and assessment [67]. Craniovertebral junction pathologies both congenital and acquired alter CSF flow, which is the main cause for the development of hydrocephalus and symptoms. Improved CSF velocity in such cases after surgery are associated with favorable response. If CSF flow is seen within syringomyelic cysts, it provides a clue to the possibility of further enlargement and helps to distinguish it from myelomalacia, which is a close differential on conventional imaging [68, 69].

Chemical shift imaging (CSI) makes use of the differences in precession frequencies of lipid and water protons within the same imaging voxel acquired using different echo times. CSI leads to output where lipid and water signals are additive (in-phase) or subtracted (opposed-phase). This helps to assess vertebral bone marrow fat content in benign processes (osteoporosis, hemangiomas, degenerative endplate changes, etc.) versus malignant infiltrative processes (e.g. leukemia, lymphoma and metastasis), thereby potentially avoiding biopsy in a significant percentage of patients. Signal drop-out of 20% as a cut-off can be used to differentiate benign lesions from malignant lesions (Fig. 4.25) [80–83]. CSI can also be used to differentiate vertebral compression fractures of benign from malignant etiologies [84].

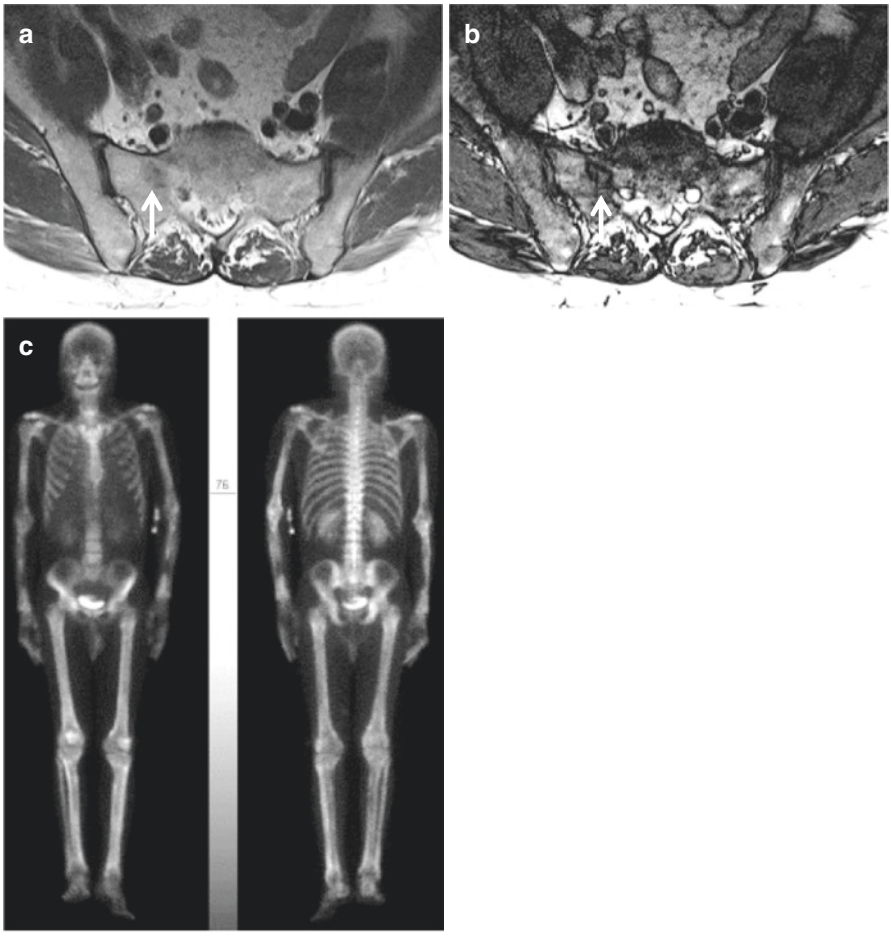

Fig. 4.25 Focal lesion in Midline of sacrum (**a**) Shows In-phase image with altered signal, (**b**) Shows Out-of-phase image with loss of signal of more than 20% in corresponding area. and (**c**) Shows bone scan without corresponding uptake. This lesion was unchanged over years and was classified as focal red marrow conversion

MR perfusion-weighted imaging (PWI) assesses the amount of blood flow into tissues and thus, also assesses biologic behavior of neoplasms, identifies ischemic/infarcted regions and aids in characterization of other lesions/diseases. Perfusion MRI techniques can be done with or without using an exogenous contrast agent. Dynamic susceptibility contrast (DSC) assesses signal loss in T2 or T2* by the passage of the bolus of contrast agent through the tissue. Dynamic contrast enhanced (DCE) assesses increase in signal on T1 before and after passage of the bolus of contrast agent in the tissue. Without using contrast, arterial spin-labeling (ASL) assesses magnetically labeled blood on T1 to estimate perfusion. ASL can be used as pulsed or continuous. ASL is used to assess cerebral blood flow (CBF) and takes about 5–8 min to acquire. ASL has also been used experimentally in patients with discogenic pain and to evaluate vascularity of spinal tumors. PWI has thus been used to assess spinal neoplasm - primary malignant, metastatic lesions, and benign lesions like hemangioblastoma to evaluate tumor biology and vascularity. PWI also been used to predict outcomes of spinal lesions with encouraging results [85]. Using perfusion studies, ischemia and hypoxia has been studied in the pathogenesis of myelopathy and to suggest early intervention to prevent full blown myelopathy and future disability [86].

Future Directions

Extensive research is happening at a faster pace in various parts of the world, bringing newer technologies and uses in spinal imaging for a variety of pathologies. To mention a few, Paraspinal Muscle and extremity muscle segmentation on CT or MRI using automated computer software with Atlas-based tools. Apart from muscle bulk measurement, it also provides information about the amount of fatty infiltration. Manual annotation of the muscles is time-consuming and laborious. Automated pseudo-coloring technique or histogram analysis would likely lead to easy and accurate assessment of the different muscles and its pathologies [87]. The surrogate quantitative imaging markers can serve as treatment response and prognostic indicators.

Artificial intelligence has been tried in spine fracture detection on plain radiographs. With everyday improving robust and powerful computational power, the deep neural networks will become more advanced and there will be an extraordinary change, the way imaging is being interpreted and used. Mundane and repeated tasks can be accomplished by machine and the imaging interpretations of specific tasks, e.g. spine fracture or detection of compression fracture, will likely be done in an equivalent manner to expert radiologists. This will especially help medical care in remote locations, aiding in timely management of trauma and other patients [88, 89]. Artificial intelligence has also been shown to predict fractures in predisposed patients [90].

Role of Magnetization Transfer MRI, Diffusion Tensor Imaging, Diffusion non-Tensor Imaging (q-space), Myelin Water Imaging, fMRI and Perfusion in detailed evaluation of spinal cord in trauma are also being investigated [91]. Functional MRI

has been tried in spinal cord similar to what has been already established in brain imaging [92]. Diffusion tensor imaging (DTI) has been employed to assess microstructure of muscle tissue in its physiological and pathological stages. Thus, track subtle changes of muscle tissue composition especially in important muscles like back muscles. These strategies are being aimed at early interventions that can prevent occurrence or help better treat related pathologies affecting these muscles [93]. Dixon based fatty changes in muscles are shown equivalent to MR spectroscopy, a metabolic imaging quantitative technique [94].

Multiple studies have shown the application of Hybrid SPECT with CT fusion to identify potential sites for treatment in patients with axial neck and back pain. Presurgical assessment for hypermetabolic foci on spinal SPECT imaging correlating with back pain sites and similar post-operative assessment have been show to produce better outcomes in early investigations [95].

ASL can be used to assess marrow perfusion and hence biological changes within the bones. It might have role in finding bone loss, fatty conversion, directing interventions, and evaluate therapy response and prognosis based on perfusion changes [96].

To conclude, radiologic imaging of spine has come a long way with many advanced techniques being currently in use and many on horizon. Gaining understanding of optimal indications of different imaging modalities is essential for a reader to prudently apply these technologies in their practice for the benefit of patients.

Disclosures AC serves as a consultant for ICON Medical and Treace Medical Concepts Inc. AC receives royalties from Jaypee and Wolters.

Conflicts of Interest None.

References

1. Gillis L. Cineradiography in orthopaedic surgery. Br Med J. 1947;2(4516):140.
2. Hoeffner EG, Mukherji SK, Srinivasan A, Quint DJ. Neuroradiology back to the future: spine imaging. AJNR Am J Neuroradiol. 2012;33(6):999–1006.
3. Nouh MR. Imaging of the spine: where do we stand? World J Radiol. 2019;11(4):55–61.
4. Davis MA. Where the united states spends its spine dollars: Expenditures on different ambulatory services for the management of back and neck conditions. Spine. 2012;37(19):1693–701.
5. Libson E, Bloom RA, Dinari G, Robin GC. Oblique lumbar spine radiographs: importance in young patients. Radiology. 1984;151(1):89–90.
6. West OC, Anbari MM, Pilgram TK, Wilson AJ. Acute cervical spine trauma: diagnostic performance of single-view versus three-view radiographic screening. Radiology. 1997;204(3):819–23.
7. Jumah F, Alkhdour S, Mansour S, He P, Hroub A, Adeeb N, et al. Os odontoideum: a comprehensive clinical and surgical review. Cureus. 2017;9(8):e1551.
8. Electricwala AJ, Harsule A, Chavan V, Electricwala JT. Complete atlantooccipital assimilation with basilar invagination and atlantoaxial subluxation treated non-surgically: a case report. Cureus. 2017;9(6):e1327.

9. Donnally III CJ, Munakomi S, Varacallo M. Basilar invagination. In: StatPearls [Internet]. Treasure Island (FL): StatPearls Publishing; 2020 [cited 2020 Aug 9]. Available from: http://www.ncbi.nlm.nih.gov/books/NBK448153/.
10. Smoker WR. Craniovertebral junction: normal anatomy, craniometry, and congenital anomalies. Radiographics. 1994;14(2):255–77.
11. Denis F. The three column spine and its significance in the classification of acute thoracolumbar spinal injuries. Spine. 1983;8(8):817–31.
12. Haher TR, Tozzi JM, Lospinuso MF, Devlin V, O'Brien M, Tenant R, et al. The contribution of the three columns of the spine to spinal stability: a biomechanical model. Paraplegia. 1989;27(6):432–9.
13. Kim H, Kim HS, Moon ES, Yoon C-S, Chung T-S, Song H-T, et al. Scoliosis imaging: what radiologists should know. Radiographics. 2010;30(7):1823–42.
14. Hasegawa K, Okamoto M, Hatsushikano S, Caseiro G, Watanabe K. Difference in whole spinal alignment between supine and standing positions in patients with adult spinal deformity using a new comparison method with slot-scanning three-dimensional X-ray imager and computed tomography through digital reconstructed radiography. BMC Musculoskelet Disord [Internet]. 2018 Dec 6 [cited 2020 May 26];19. Available from: https://www.ncbi.nlm.nih.gov/pmc/articles/PMC6284293/.
15. Ahmadi A, Maroufi N, Behtash H, Zekavat H, Parnianpour M. Kinematic analysis of dynamic lumbar motion in patients with lumbar segmental instability using digital videofluoroscopy. Eur Spine J. 2009;18(11):1677–85.
16. Harris TJ, Blackmore CC, Mirza SK, Jurkovich GJ. Clearing the cervical spine in obtunded patients. Spine. 2008;33(14):1547–53.
17. Como JJ, Diaz JJ, Dunham CM, Chiu WC, Duane TM, Capella JM, et al. Practice management guidelines for identification of cervical spine injuries following trauma: update from the eastern association for the surgery of trauma practice management guidelines committee. J Trauma. 2009;67(3):651–9.
18. Padayachee L, Cooper DJ, Irons S, Ackland HM, Thomson K, Rosenfeld J, et al. Cervical spine clearance in unconscious traumatic brain injury patients: dynamic flexion-extension fluoroscopy versus computed tomography with three-dimensional reconstruction. J Trauma. 2006;60(2):341–5.
19. Schueler BA. The AAPM/RSNA physics tutorial for residents: general overview of fluoroscopic imaging. Radiographics. 2000;20(4):1115–26.
20. Koslowski L, Weller S. The application of x-ray image intensification to orthopaedic surgery. Ger Med Mon. 1966;11(2):61–2.
21. Berci G, Zheutlin N. Improving radiology in surgery. Med Instrum. 1976;10(2):110–4.
22. Kausch L, Thomas S, Kunze H, Privalov M, Vetter S, Franke J, et al. Toward automatic C-arm positioning for standard projections in orthopedic surgery. Int J Comput Assist Radiol Surg. 2020;15(7):1095–105.
23. Magerl FP. Stabilization of the lower thoracic and lumbar spine with external skeletal fixation. Clin Orthop. 1984;189:125–41.
24. Herscovici D, Sanders RW. The effects, risks, and guidelines for radiation use in orthopaedic surgery. Clin Orthop. 2000;375:126–32.
25. Salvia JCL, de Moraes PR, Ammar TY, Schwartsmann CR. Fluoroscopy duration in orthopedic surgery. Rev Bras Ortop. 2011;46(2):136–8.
26. Narain AS, Hijji FY, Yom KH, Kudaravalli KT, Haws BE, Singh K. Radiation exposure and reduction in the operating room: perspectives and future directions in spine surgery. World J Orthop. 2017;8(7):524–30.
27. Hott JS, Papadopoulos SM, Theodore N, Dickman CA, Sonntag VKH. Intraoperative Iso-C C-arm navigation in cervical spinal surgery: review of the first 52 cases. Spine. 2004;29(24):2856–60.
28. Kim CW, Lee Y-P, Taylor W, Oygar A, Kim WK. Use of navigation-assisted fluoroscopy to decrease radiation exposure during minimally invasive spine surgery. Spine J. 2008;8(4):584–90.

29. Smith HE, Welsch MD, Sasso RC, Vaccaro AR. Comparison of radiation exposure in lumbar pedicle screw placement with fluoroscopy vs computer-assisted image guidance with intraoperative three-dimensional imaging. J Spinal Cord Med. 2008;31(5):532–7.
30. Husseini JS, Simeone FJ, Staffa SJ, Palmer WE, Chang CY. Fluoroscopically guided lumbar spine interlaminar and transforaminal epidural injections: inadvertent intravascular injection. Acta Radiol. 2020;61(11):1534–40.
31. Engel A, King W, MacVicar J, Standards Division of the International Spine Intervention Society. The effectiveness and risks of fluoroscopically guided cervical transforaminal injections of steroids: a systematic review with comprehensive analysis of the published data. Pain Med. 2014;15(3):386–402.
32. Cyteval C, Thomas E, Decoux E, Sarrabere M-P, Cottin A, Blotman F, et al. Cervical radiculopathy: open study on percutaneous periradicular foraminal steroid infiltration performed under CT control in 30 patients. AJNR Am J Neuroradiol. 2004;25(3):441–5.
33. Depriester C, Setbon S, Larde A, Malaquin E, Vanden Abeele B, Bocquet J. CT-guided transforaminal cervical and lumbar epidural injections. Diagn Interv Imaging. 2012;93(9):704–10.
34. Wald JT, Maus TP, Geske JR, Carter RE, Diehn FE, Kaufmann TJ, et al. Safety and efficacy of CT-guided transforaminal cervical epidural steroid injections using a posterior approach. AJNR Am J Neuroradiol. 2012;33(3):415–9.
35. Gossner J. Safety of CT-guided lumbar nerve root infiltrations. Analysis of a two-year period. Interv Neuroradiol. 2014;20(5):533–7.
36. Gangi A, Guth S, Imbert JP, Marin H, Dietemann J-L. Percutaneous vertebroplasty: indications, technique, and results. Radiographics. 2003;23(2):e10.
37. Bernard TN. Lumbar discography followed by computed tomography. Refining the diagnosis of low-back pain. Spine. 1990;15(7):690–707.
38. McCutcheon ME, Thompson WC. CT scanning of lumbar discography. A useful diagnostic adjunct. Spine. 1986;11(3):257–9.
39. Kluner C, Kivelitz D, Rogalla P, Putzier M, Hamm B, Enzweiler C. Percutaneous discography: comparison of low-dose CT, fluoroscopy and MRI in the diagnosis of lumbar disc disruption. Eur Spine J. 2006;15(5):620–6.
40. Walker J, El Abd O, Isaac Z, Muzin S. Discography in practice: a clinical and historical review. Curr Rev Musculoskelet Med. 2008;1(2):69–83.
41. Roos JE, Hilfiker P, Platz A, Desbiolles L, Boehm T, Marincek B, et al. MDCT in emergency radiology: is a standardized chest or abdominal protocol sufficient for evaluation of thoracic and lumbar spine trauma? AJR Am J Roentgenol. 2004;183(4):959–68.
42. Raniga SB, Skalski MR, Kirwadi A, Menon VK, Al-Azri FH, Butt S. Thoracolumbar spine injury at CT: trauma/emergency radiology. Radiographics. 2016;36(7):2234–5.
43. Ghodasara N, Yi PH, Clark K, Fishman EK, Farshad M, Fritz J. Postoperative spinal CT: what the radiologist needs to know. Radiographics. 2019;39(6):1840–61.
44. Ospina Moreno C, Vela Marín AC, Castán Senar A, Montejo Gañán I, Cózar Bartos M, Marín Cárdenas MA. Radiological diagnosis of spinal arachnoid cysts: a pictorial essay. J Med Imaging Radiat Oncol. 2016;60(5):632–8.
45. Patel DM, Weinberg BD, Hoch MJ. CT myelography: clinical indications and imaging findings. Radiographics. 2020;40(2):470–84.
46. Song K-J, Choi B-W, Kim G-H, Kim J-R. Clinical usefulness of CT-myelogram comparing with the MRI in degenerative cervical spinal disorders: is CTM still useful for primary diagnostic tool? J Spinal Disord Tech. 2009;22(5):353–7.
47. Chazen JL, Talbott JF, Lantos JE, Dillon WP. MR myelography for identification of spinal CSF leak in spontaneous intracranial hypotension. AJNR Am J Neuroradiol. 2014;35(10):2007–12.
48. Luetmer PH, Schwartz KM, Eckel LJ, Hunt CH, Carter RE, Diehn FE. When should I do dynamic CT myelography? Predicting fast spinal CSF leaks in patients with spontaneous intracranial hypotension. AJNR Am J Neuroradiol. 2012;33(4):690–4.
49. Taurog JD, Chhabra A, Colbert RA. Ankylosing spondylitis and axial spondyloarthritis. N Engl J Med. 2016;374(26):2563–74.

50. Alian A, Omar H, Chhabra A. Cross-sectional imaging for inflammatory arthropathy of the pelvis. Semin Ultrasound CT MR. 2017;38(3):279–90.
51. Ruiz-Gaviria R, Baracaldo I, Castañeda C, Ruiz-Patiño A, Acosta-Hernandez A, Rosselli D. Specificity and sensitivity of aquaporin 4 antibody detection tests in patients with neuromyelitis optica: a meta-analysis. Mult Scler Relat Disord. 2015;4(4):345–9.
52. Chhabra A, Ezzati F, Taurog JD, Xi Y, Pezeshk P. Three tesla and 3D multiparametric combined imaging evaluation of axial spondyloarthritis and pelvic enthesopathy. Eur J Radiol. 2020;126:108916.
53. Sanal HT, Yilmaz S, Kalyoncu U, Cinar M, Simsek I, Erdem H, et al. Value of DWI in visual assessment of activity of sacroiliitis in longstanding ankylosing spondylitis patients. Skelet Radiol. 2013;42(2):289–93.
54. Zhao Y, Li S, Liu Z, Chen X, Zhao X, Hu S, et al. Detection of active sacroiliitis with ankylosing spondylitis through intravoxel incoherent motion diffusion-weighted MR imaging. Eur Radiol. 2015;25(9):2754–63.
55. Dreghorn CR, Newman RJ, Hardy GJ, Dickson RA. Primary tumors of the axial skeleton. Experience of the Leeds Regional Bone Tumor Registry. Spine. 1990;15(2):137–40.
56. Schellinger KA, Propp JM, Villano JL, McCarthy BJ. Descriptive epidemiology of primary spinal cord tumors. J Neuro-Oncol. 2008;87(2):173–9.
57. Krings T, Lasjaunias PL, Hans FJ, Mull M, Nijenhuis RJ, Alvarez H, et al. Imaging in spinal vascular disease. Neuroimaging Clin N Am. 2007;17(1):57–72.
58. Trenga AP, Singla A, Feger MA, Abel MF. Patterns of congenital bony spinal deformity and associated neural anomalies on X-ray and magnetic resonance imaging. J Child Orthop. 2016;10(4):343–52.
59. Alexander PG, Tuan RS. Role of environmental factors in axial skeletal dysmorphogenesis. Birth Defects Res C Embryo Today. 2010;90(2):118–32.
60. Soldatos T, Chalian M, Thawait S, Belzberg AJ, Eng J, Carrino JA, et al. Spectrum of magnetic resonance imaging findings in congenital lumbar spinal stenosis. World J Clin Cases. 2014;2(12):883–7.
61. Nagaraj UD, Bierbrauer KS, Peiro JL, Kline-Fath BM. Differentiating closed versus open spinal dysraphisms on fetal MRI. AJR Am J Roentgenol. 2016;207(6):1316–23.
62. Nacar Dogan S, Kizilkilic O, Kocak B, Isler C, Islak C, Kocer N. Intrathecal gadolinium-enhanced MR cisternography in patients with otorhinorrhea: 10-year experience of a tertiary referral center. Neuroradiology. 2018;60(5):471–7.
63. Hansen BB. Introducing standing weight-bearing MRI in the diagnostics of low back pain and degenerative spinal disorders. Dan Med J. 2017;64(10):B5416.
64. Hansen BB, Nordberg CL, Hansen P, Bliddal H, Griffith JF, Fournier G, et al. Weight-bearing MRI of the lumbar spine: spinal stenosis and spondylolisthesis. Semin Musculoskelet Radiol. 2019;23(6):621–33.
65. Ferreiro Perez A, Garcia Isidro M, Ayerbe E, Castedo J, Jinkins JR. Evaluation of intervertebral disc herniation and hypermobile intersegmental instability in symptomatic adult patients undergoing recumbent and upright MRI of the cervical or lumbosacral spines. Eur J Radiol. 2007;62(3):444–8.
66. Gilbert JW, Martin JC, Wheeler GR, Storey BB, Mick GE, Richardson GB, et al. Lumbar disk protrusion rates of symptomatic patients using magnetic resonance imaging. J Manip Physiol Ther. 2010;33(8):626–9.
67. Meakin JR, Smith FW, Gilbert FJ, Aspden RM. The effect of axial load on the sagittal plane curvature of the upright human spine in vivo. J Biomech. 2008;41(13):2850–4.
68. Tarantino U, Fanucci E, Iundusi R, Celi M, Altobelli S, Gasbarra E, et al. Lumbar spine MRI in upright position for diagnosing acute and chronic low back pain: statistical analysis of morphological changes. J Orthop Traumatol. 2013;14(1):15–22.
69. Park GE, Jee W-H, Lee S-Y, Sung J-K, Jung J-Y, Grimm R, et al. Differentiation of multiple myeloma and metastases: use of axial diffusion-weighted MR imaging in addition to standard MR imaging at 3T. PLoS One. 2018;13(12):e0208860.

70. Daghighi MH, Poureisa M, Safarpour M, Behzadmehr R, Fouladi DF, Meshkini A, et al. Diffusion-weighted magnetic resonance imaging in differentiating acute infectious spondylitis from degenerative Modic type 1 change; the role of b-value, apparent diffusion coefficient, claw sign and amorphous increased signal. Br J Radiol. 2016;89(1066):20150152.
71. Dumont RA, Keen NN, Bloomer CW, Schwartz BS, Talbott J, Clark AJ, et al. Clinical utility of diffusion-weighted imaging in spinal infections. Clin Neuroradiol. 2019;29(3):515–22.
72. Drake-Pérez M, Boto J, Fitsiori A, Lovblad K, Vargas MI. Clinical applications of diffusion weighted imaging in neuroradiology. Insights Imaging. 2018;9(4):535–47.
73. Bozgeyik Z, Ozgocmen S, Kocakoc E. Role of diffusion-weighted MRI in the detection of early active sacroiliitis. AJR Am J Roentgenol. 2008;191(4):980–6.
74. Chhabra A, Zhao L, Carrino JA, Trueblood E, Koceski S, Shteriev F, et al. MR neurography: advances. Radiol Res Pract. 2013;2013:809568.
75. Chhabra A, Andreisek G, Soldatos T, Wang KC, Flammang AJ, Belzberg AJ, et al. MR neurography: past, present, and future. AJR Am J Roentgenol. 2011;197(3):583–91.
76. Chhabra A, Thawait GK, Soldatos T, Thakkar RS, Del Grande F, Chalian M, et al. High-resolution 3T MR neurography of the brachial plexus and its branches, with emphasis on 3D imaging. AJNR Am J Neuroradiol. 2013;34(3):486–97.
77. Soldatos T, Andreisek G, Thawait GK, Guggenberger R, Williams EH, Carrino JA, et al. High-resolution 3-T MR neurography of the lumbosacral plexus. Radiographics. 2013;33(4):967–87.
78. Hwang L, Dessouky R, Xi Y, Amirlak B, Chhabra A. MR neurography of greater occipital nerve neuropathy: initial experience in patients with migraine. AJNR Am J Neuroradiol. 2017;38(11):2203–9.
79. Dessouky R, Khaleel M, Khalifa DN, Tantawy HI, Chhabra A. Magnetic resonance neurography of the lumbosacral plexus in failed back surgery syndrome. Spine. 2018;43(12):839–47.
80. Zampa V, Cosottini M, Michelassi C, Ortori S, Bruschini L, Bartolozzi C. Value of opposed-phase gradient-echo technique in distinguishing between benign and malignant vertebral lesions. Eur Radiol. 2002;12(7):1811–8.
81. Douis H, Davies AM, Jeys L, Sian P. Chemical shift MRI can aid in the diagnosis of indeterminate skeletal lesions of the spine. Eur Radiol. 2016;26(4):932–40.
82. Suh CH, Yun SJ, Jin W, Park SY, Ryu C-W, Lee SH. Diagnostic performance of in-phase and opposed-phase chemical-shift imaging for differentiating benign and malignant vertebral marrow lesions: a meta-analysis. AJR Am J Roentgenol. 2018;211(4):W188–97.
83. Pezeshk P, Alian A, Chhabra A. Role of chemical shift and Dixon based techniques in musculoskeletal MR imaging. Eur J Radiol. 2017;94:93–100.
84. Eito K, Waka S, Naoko N, Makoto A, Atsuko H. Vertebral neoplastic compression fractures: assessment by dual-phase chemical shift imaging. J Magn Reson Imaging. 2004;20(6):1020–4.
85. Jahng G-H, Li K-L, Ostergaard L, Calamante F. Perfusion magnetic resonance imaging: a comprehensive update on principles and techniques. Korean J Radiol. 2014;15(5):554–77.
86. Ellingson BM, Woodworth DC, Leu K, Salamon N, Holly LT. Spinal cord perfusion MR imaging implicates both ischemia and hypoxia in the pathogenesis of cervical spondylosis. World Neurosurg. 2019;128:e773–81.
87. Li H, Luo H, Liu Y. Paraspinal muscle segmentation based on deep neural network. Sensors. 2019;19(12):2650.
88. Kim DH, MacKinnon T. Artificial intelligence in fracture detection: transfer learning from deep convolutional neural networks. Clin Radiol. 2018;73(5):439–45.
89. Cheng C-T, Ho T-Y, Lee T-Y, Chang C-C, Chou C-C, Chen C-C, et al. Application of a deep learning algorithm for detection and visualization of hip fractures on plain pelvic radiographs. Eur Radiol. 2019;29(10):5469–77.
90. Badgeley MA, Zech JR, Oakden-Rayner L, Glicksberg BS, Liu M, Gale W, et al. Deep learning predicts hip fracture using confounding patient and healthcare variables. NPJ Digit Med. 2019;2:31.
91. Smith SA, Pekar JJ, van Zijl PCM. Advanced MRI strategies for assessing spinal cord injury. Handb Clin Neurol. 2012;109:85–101.

92. Choe AS. Advances in spinal functional magnetic resonance imaging in the healthy and injured spinal cords. Curr Phys Med Rehabil Rep. 2017;5(3):143–50.
93. Klupp E, Cervantes B, Schlaeger S, Inhuber S, Kreuzpointer F, Schwirtz A, et al. Paraspinal muscle DTI metrics predict muscle strength. J Magn Reson Imaging. 2019;50(3):816–23.
94. Fischer MA, Nanz D, Shimakawa A, Schirmer T, Guggenberger R, Chhabra A, et al. Quantification of muscle fat in patients with low back pain: comparison of multi-echo MR imaging with single-voxel MR spectroscopy. Radiology. 2013;266(2):555–63.
95. Brusko GD, Perez-Roman RJ, Tapamo H, Burks SS, Serafini AN, Wang MY. Preoperative SPECT imaging as a tool for surgical planning in patients with axial neck and back pain. Neurosurg Focus. 2019;47(6):E19.
96. Xing D, Zha Y, Yan L, Wang K, Gong W, Lin H. Feasibility of ASL spinal bone marrow perfusion imaging with optimized inversion time. J Magn Reson Imaging. 2015;42(5):1314–20.